Title: Topical application of a BCL-2 inhibitor ameliorates imiquimod-induced psoriasiform dermatitis by eliminating senescent cells

Authors: Huan Zhu[*1], Jiao Jiang[*1, 2], Ming Yang[1], Mingming Zhao[1], Zhenghao He[1], Congli Tang[3], Cailing Song[4], Ming Zhao[1], Arne N. Akbar[5], Venkat Reddy[6], Wenjing Pan[4], Song Li[4], Yixin Tan[1], Haijing Wu[#1], and Qianjin Lu[#1, 2]

Affiliations:

[1] Department of Dermatology, Hunan Key Laboratory of Medical Epigenomics, The Second Xiangya Hospital of Central South University, Changsha, Hunan, China.

[2] Hospital for Skin Diseases, Institute of Dermatology, Chinese Academy of Medical Sciences & Peking Union Medical College, Nanjing, Jiangsu, China.

[3] State Key Laboratory of Bioelectronics, Southeast University, Nanjing, Jiangsu, China.

[4] Hunan Key Laboratory of Biomedical Nanomaterials and Devices, Hunan University of Technology, Zhuzhou, Hunan, China.

[5] Division of Medicine, University College London, London, WC1E 6JF, United Kingdom.

[6] Centre for Rheumatology, Division of Medicine, University College London, London, WC1E 6JF, United Kingdom.

[#] Address correspondence to Haijing Wu, The Second Xiangya Hospital of Central South University, 139 Renmin Middle Road, Changsha, Hunan 410011, China. Phone: +86-731-

85294099; Email: chriswu1010@csu.edu.cn. Or to: Qianjin Lu, The Second Xiangya Hospital of Central South University, 139 Renmin Middle Road, Changsha, Hunan 410011, China. Phone: +86-731-85295860; Email: qianlu5860@pumcderm.cams.cn.

*These authors contributed equally to this work.

Funding: This work was supported by National Natural Science Foundation of China (No. 81830097, No. 82273540, No. 81972943, No. 82173425); Special Program of National Natural Science Foundation of China (No. 32141004); National Science and Technology Major Project (No. 2020ZX09201-28); Hunan Talent Young Investigator (No. 2019RS2012); Hunan Outstanding Young Investigator (No. 2020JJ2055); CAMS Innovation Fund for Medical Sciences (CIFMS) (No. 2021-I2M-1-059); National Key R&D Program of China (No.2022YFC3601800, No.2021YFC2702004), and Central South University Innovation-Driven Research Programme (No. 2023CXQD046). Non-profit Central Research Institute Fund of Chinese Academy of Medical Sciences (No.2020-RC320-003).

Competing Interests: The authors have no relevant financial or non-financial interests to disclose.

Text word count: 3095, number of references: 50, tables: 0, and figures: 6.

Abstract

Background: Psoriasis is an inflammatory skin disease with unclear pathogenesis and unmet therapeutic needs.

Objective: To investigate the role of senescent $CD4^+$ T cells in psoriatic lesion formation and explore the application of senolytics in treating psoriasis.

Methods: We explored the expression levels of $p16^{INK4a}$ and p21, classical markers of cellular senescence, in $CD4^+$ T cells from human psoriatic lesions and imiquimod (IMQ)-induced psoriatic lesions. We prepared a senolytic gel using B-cell lymphoma 2 (BCL-2) inhibitor ABT-737 and evaluated its therapeutic efficacy in treating psoriasis.

Results: Using multispectrum immunohistochemistry (mIHC) staining, we detected increased expression levels of $p16^{INK4a}$ and p21 in $CD4^+$ T cells from psoriatic lesions. After topical application of ABT-737 gel, significant alleviation of IMQ-induced psoriatic lesions was observed, with milder pathological alterations. Mechanistically, ABT-737 gel significantly decreased the percentage of senescent cells, expression of T cell receptor (TCR) α and β chains, and expression of *Tet methylcytosine dioxygenase 2* (*Tet2*) in IMQ-induced psoriatic lesions, as determined by mIHC, high-throughput sequencing of the TCR repertoire, and RT-qPCR, respectively. Furthermore, the severity of psoriatic lesions in $CD4^{cre}Tet2^{f/f}$ mice was milder than that in $Tet2^{f/f}$ mice in the IMQ-induced psoriasis model.

Conclusion: We revealed the roles of senescent $CD4^+$ T cells in developing psoriasis and highlighted the therapeutic potential of topical ABT-737 gel in treating psoriasis through

the elimination of senescent cells, modulation of the TCR α β repertoire, and regulation of the TET2-Th17 cell pathway.

Keywords psoriasis, cellular senescence, senolytics, BCL-2 inhibitor.

Introduction

Psoriasis is an inflammatory skin disorder characterized by pruritus, erythema and scales on body areas [1]. The inflammatory response in psoriatic lesions is mainly initiated by interactions among keratinocytes, dendritic cells, and $CD4^+$ T cells through the IL-23/IL-17/IL-22 axis and subsequent inflammatory cascades [1-3]. Current treatments for psoriasis, including glucocorticoids and immunosuppressants, often have undesirable side effects, such as leucopenia and infection[5]. Therefore, studies investigating the fundamental mechanisms underlying psoriasis and exploring new therapies are urgently needed.

Cellular senescence refers to permanent cell cycle arrest triggered by both for self-protection caused by exogenous and endogenous cellular stresses, such as radiation, repetitive cell replication, and mitochondrial dysregulation [9, 10]. Typical characteristics of senescent cells include the increased cyclin-dependent kinase inhibitors $p16^{INK4a}$ and p21, excessive senescence-associated secretory phenotype (SASPs), as well as antiapoptotic proteins [11]. The antiapoptotic protein BCL-2 is the major regulator of mitochondrial apoptosis through the control of mitochondrial outer membrane permeabilization (MOMP) [12, 13]. Multiple findings suggest a strong association between BCL-2 and cellular senescence. On the one hand, BCL-2 expression can induce cellular senescence[14], as it can accelerate the oncogenic Ras-induced senescence program and promote senescence triggered by DNA damage and starvation through p38 MAPK activation [15, 16]. On the other hand, senescent cells exhibit resistance to apoptosis, primarily due to increased transcription levels of BCL-2 [14]. The increase in BCL-2 in senescent cells promotes cell cycle arrest and apoptosis resistance by upregulating cyclin-dependent proteins (p27 and

p130) as well as inhibiting apoptosis, ultimately leading to the accumulation of senescent cells [16].

Cellular senescence is involved in the pathogenesis of metabolic disorders, cardiovascular diseases, and autoimmune diseases. Therapies targeting senescent cells, known as senolytics, have been investigated as potential treatments for many disorders [10, 11, 17]. ABT-737 and ABT-263, inhibitors of BCL-2, BCL-xL, and BCL-w, possess proapoptotic properties and are currently being investigated in preclinical studies and clinical trials for hematological cancers [18]. Recently, ABT-737 and ABT-263 were explored as senolytic drugs capable of eliminating senescent cells, potentially delaying the progression of liver regeneration disorders, diabetes, and other diseases [19-24]. Despite the widespread application of BCL-2 inhibitors, their commonly employed delivery methods, including injection and oral intake, are accompanied by poor compliance and unexpected side effects, such as diarrhea, weight loss, and platelet toxicity [25]. Herein, we investigated the role of senescent $CD4^+$ T cells in psoriasis and the potential application of senolytics in the treatment of psoriasis.

Materials and Methods

Methods and materials are described in supplementary material.

Results

1. Increased percentages of senescent CD4$^+$ p16^{INK4a+} and CD4$^+$ p21$^+$ T cells in human psoriatic lesions.

The cyclin-dependent kinase inhibitors p16^{INK4a} and p21 are considered crucial markers of cellular senescence [11]. Using multispectrum immunohistochemistry (mIHC) staining, we observed higher levels of p16^{INK4a} and p21 in the epidermis and dermis of psoriasis patients compared to healthy controls (HCs) (Figure 1A-1B). We also observed increased percentages of CD4$^+$ p16^{INK4a+} T cells and CD4$^+$ p21$^+$ T cells in psoriatic dermis (Figure 1C-1D). Besides, flow cytometry analysis confirmed that the frequencies of p16^{INK4a+} and p21$^+$ CD4$^+$ T cells in human psoriatic lesions were greater than those in HCs (Figure 1E-1F).

Previous studies have indicated that elevated BCL-2 and BCL-xL expression is a defense mechanism against apoptosis in senescent cells [19, 20, 26]. Therapies targeting BCL-xL have been shown to eliminate senescent cells and ameliorate many diseases [19-24]. Herein, we determined the percentages of BCL-2 and BCL-xL$^+$ cells in psoriatic lesions using mIHC staining and observed increased frequency of BCL-xL$^+$p16^{INK4a+} cells in the epidermis and CD4$^+$BCL-2$^+$ cells in the dermis of patients with psoriasis (Figure 1G-1H). These findings indicated that senescent cells in human psoriasis lesions may upregulate the protein expression of BCL-2 and BCL-xL to escape apoptosis and exert pathogenic effects. Thus, BCL-2 and BCL-xL may hold promise as therapeutic targets for treating psoriasis by reducing senescent cells.

2. **Topical application of ABT-737 ameliorates IMQ-induced psoriasis-like lesions.**

We evaluated the level of cellular senescence in a commonly used IMQ-induced psoriatic mouse model [27],.and observed similar results that are comparable to those observed in psoriasis patients. The percentages of $p16^{INK4a+}$ cells, $p21^{+}$ cells, BCL-2^{+} cells, and BCL-xL^{+} cells, were greater in IMQ-induced psoriatic lesions than in normal controls (NCs) (Figure S1). Thus, we used IMQ-induced psoriatic mouse model to investigate the therapeutic role of the BCL-2 inhibitor ABT-737 in the treatment of psoriasis. Instead of traditional delivery methods such as intraperitoneal injection or oral intake, we developed novel topical delivery methods for the treatment: subcutaneous injection and topical gel.

For the subcutaneous injection of ABT-737, we subcutaneously injected a daily dose of 25 mg/kg ABT-737 or an equivalent amount of vehicle into the shaved backs of IMQ-induced psoriasis-like mouse model for 7 consecutive days. For the ABT-737 gel treatment, we applied a daily topical dose of 0.5 g of ABT-737 gel (0.5‰ concentration) or equivalent vehicle gel on shaved backs of mice for one week. Both the ABT-737 injection group and ABT-737 gel group showed significant alleviation of psoriatic lesions, manifesting as reduced erythema, scales, and thickening (Figure 2A). H&E staining revealed that pathological characteristics also significantly improved, with milder thickening and acanthosis and less dermal inflammatory cell infiltration, after subcutaneous injections of ABT-737 or the topical application of ABT-737 gel (Figure 2B). Both the psoriasis area severity index (PASI) scores and epidermal thickness significantly decreased after two applications of ABT-737 (Figure 2C-2D).

Moreover, reduced expression of BCL-2 and BCL-xL were found in IMQ-induced psoriatic lesions after the topical application of ABT-737 gel (Figure 2E-2F). This result indicated good absorption and satisfactory effects of ABT-737 gel in inhibiting BCL-2 and BCL-xL expression in the skin. In addition, considering the potential inconvenience and discomfort associated with subcutaneous injections, ABT-737 gel represents a more acceptable, convenient, and painless method. Thus, the ABT-737 gel was further explored in subsequent experiments to determine its efficacy, safety profile, and underlying mechanisms of action.

3. ABT-737 gel treatment significantly reduced the frequency of senescent $CD4^+$ T cells and decreased the mRNA expression levels of inflammatory cytokines and SASPs in IMQ-induced psoriasis-like lesions.

We performed mIHC staining to determine the frequencies of $p16^{INK4a+}$ cells and $p21^+$ cells in IMQ-induced psoriatic lesions in BALB/c mice to evaluate the ability of topically applied ABT-737 gel to eliminate senescent cells. The percentages of $p16^{INK4a+}$ cells and $p21^+$ cells significantly decreased after the topical application of ABT-737 gel (Figure 3A-3B). These results were confirmed through RT–qPCR analysis (Figure 3C). After topical application of ABT-737 gel, the percentages of $CD4^+$ $p16^{INK4a+}$ and $CD4^+$ $p21^+$ T cells decreased in dermis of psoriatic lesions (Figure 3A and 3D).

The global transcriptomic profiles of skin cells were generated by RNA sequencing to confirm the effects of the topically applied ABT-737 gel on IMQ-induced psoriatic lesions. We found that 224 genes were downregulated and 210 genes were upregulated in IMQ-

induced psoriatic lesions treated topically with the ABT-737 gel (Figure S2). Notably, the expression of genes involved in the inflammatory response (such as *Il17a*, *Il23*r, *Il18rap*, *Cd3d*, *Cd274*, *Cxcl2*, *Cxcl3*, *Cxcr5*, *Cxcl13*, *Hif1a*, *Jak3*, and *Stat5a*), cellular senescence (such as *Il1b*, *Il6*, and *Mtor*), and the BCL-2 family (such as *Bcl2a1a*, *Bcl2a1b*, and *Bcl2a1d*) was significantly downregulated following the topical application of ABT-737 gel in IMQ-induced psoriatic lesions (Figure 3E).

In addition, the mRNA expression levels of inflammatory factors associated with the pathogenesis of psoriasis, including *Il17a*, *Il17f*, *Il22*, *Il23*, and *Ifnγ*, as well as SASPs, such as *Il6* and *Tnfα*, decreased after the topical application of the ABT-737 gel to IMQ-induced psoriatic lesions (Figure 3F-3G). After the topical application of the ABT-737 gel, the mRNA expression levels of *p21* and *Tnfα* in spleen cells decreased significantly (Figure S3).

4. The ABT-737 gel decreased the expression ratio of the T-cell receptor (TCR) α and β chains in IMQ-induced psoriasis-like lesions.

Psoriasis is a T cell-mediated autoimmune skin disorder [5]. TCRs are expressed on the surface of T cell and are responsible for recognizing antigens and then transmitting signals to activate T-cell responses [28]. Immune repertoire sequencing is an advanced technology that allows for the quantitative measurement of TCR expression [29]. A previous study, through high-throughput sequencing, revealed the important role of the complementarity determining region (CDR) 3 repertoire of TCR α and TCR β chain repertoires in human psoriatic lesions [30, 31]. Herein, we investigated the effects of the ABT-737 gel on TCR chains in IMQ-induced psoriatic lesions in BALB/c mice.

We performed immune repertoire sequencing to assess the expression ratio of 4 TCRs (α, β, δ, and γ) as determined by reads or unique CDR3 sequences (uCDR3), and the percentage of TCRs in TCR repertoires in IMQ-induced psoriatic lesions. According to the number of reads, the expression ratio of the TCR α chain in skin lesions decreased significantly, and the TCR β chain showed a decreasing trend after the use of the ABT-737 gel (Figure 4A-4B). Besides, according to the uCDR3 sequences, the expression ratio of the TCR β chain also showed a decreasing trend (p =0.0586) (Figure 4C-4D). However, the percentage of cells expressing the TCR γ chain, as determined by uCDR3 sequences, increased (Figure 4C-4D). Moreover, after treatment with the ABT-737 gel, the percentage of TCR α chains in the TCR repertoire of IMQ-induced psoriatic lesions decreased significantly (Figure 4E). In summary, the the ABT-737 gel effectively reduced the expression ratio of the TCR α and β chains in mouse psoriatic lesions.

5. No systemic effects were observed in the IMQ-induced psoriasis-like model mice following treatment with the ABT-737 gel.

Recently, BCL-2 inhibitors have been studied as therapy for the treatment of solid tumors [32]. Previous studies have reported that lymphopenia and thrombocytopenia are side effects associated with ABT-737 [32, 33]. To assess the potential side effects and systemic impact of the topical application of ABT-737 gel, we analyzed the weights of the mice and the subtypes of T cells in the spleens and draining lymph nodes (DLNs). We found no significant difference in body weight (Figure 5A), total lymphocyte counts (Figure 5B) or the frequencies of Th1/Th2/Th17/Treg subsets in either the spleens (Figure 5C) or DLNs (Figure S4) of the mice treated with the ABT-737 gel or vehicle gel. These results indicated

that there were no obvious systemic effects with ABT-737 gel.

6. The ABT-737 gel reduced the expression of TET2, and the absence of TET2 in $CD4^+$ T cells alleviated IMQ-induced psoriatic lesions, as indicated by decreased numbers of senescent $CD4^+$ T cells and reduced percentages of Th1 and Th17 cells.

Tet methylcytosine dioxygenase 2 (TET2) plays a crucial role in active DNA demethylation by converting 5-methylcytosine (5-mC) into 5-hydroxymethylcytosine (5-hmC) [34]. Recently, TET2 was also reported to be associated with activate cytokine expression in Th cells [35] and cellular senescence [36, 37]. In our study, TET2 expression was greater in senescent $CD4^+$ $p21^+$ T cells from psoriatic lesions than in those from normal skin (Figure 6A-6B). Moreover, *Tet2* mRNA expression was significantly reduced in IMQ-induced psoriatic lesions after the topical application of the ABT-737 gel (Figure 3G). These results suggested that decreased TET2 expression may contribute to the elimination of senescent $CD4^+$ T cells in psoriatic lesions following the topical application of ABT-737 gel.

To confirm the direct regulation of TET2 in T cellular senescence, we performed ATAC-seq on human $CD4^+$ T cells under ABT-737 treatment, TET2 gene knockdown by small interfering RNA (siRNA), or the combination of ABT-737 with TET2 siRNA knockdown *in vitro*. Compared to siNC, TET2 exhibited a significantly decreased peak intensity in siTET2 or under ABT-737 treatment (siNC+ABT-737) (Figure S5A). Consistent with above results, the chromatin accessibility was also changed in the gene body of *Cdkn2a (encoding* $p16^{INK4a}$*),* and *Cdkn2b (encoding p15)* with the treatment of siTET2 or ABT-737 (Figure S5B). Besides, we found that the peak intensity of *Cdkn1a (encoding p21)* was also slightly

decreased by TET2 siRNA knockdown (Figure S5C). Overall, we identified TET2 and senescence-related gene alterations in chromatin-accessible regions after ABT-737 or siTET2 gene knockdown treatment. These alterations of chromatin open region may reflect the possible regulatory effects of TET2 or ABT-737 treatment on the expression of senescence-related genes.

To further investigate the role of TET2 in cellular senescence and psoriasis, we established an IMQ-induced psoriasis mouse model using $CD4^{cre}Tet2^{f/f}$ mice and $Tet2^{f/f}$ mice. As expected, compared with $Tet2^{f/f}$ mice, $CD4^{cre}Tet2^{f/f}$ mice exhibited less severe psoriatic lesions and milder pathological features according to H&E staining (Figure 6C). The frequencies of $p21^+$ cells in psoriasis-like lesions and $CD4^+$ $p21^+$ T cells among dermal cells were decreased in $CD4^{cre}Tet2^{f/f}$ mice (Figure 6D). Furthermore, the expression of cellular senescence-associated makers (such as *Cdkn1b* and *Cdkn2b)* was decreased in the skin tissues of $CD4^{cre}Tet2^{f/f}$ mice by RNA sequencing (Figure S6). RT-qPCR confirmed that the mRNA expression levels of *Tet2*, cellular senescence markers (*p16*^{INK4a}, *p21*, *Cdkn2b*, and *Mtor*), and inflammatory factors (such as *Il17a, Il17f, Il22, Il23, and Tnfα*) were dramatically decreased (Figure 6E). In addition, flow cytometry analysis revealed lower proportions of Th1 and Th17 cells in the spleens of $CD4^{cre}Tet2^{f/f}$ mice than in those of $Tet2^{f/f}$ mice (Figure 6F). The conditional knockout of Tet2 in $CD4^+$ T cells reduced the number of senescent $CD4^+$ T cells, decreased the mRNA expression levels of inflammatory factors, and diminished disease activity in an IMQ-induced psoriatic mouse model. Therefore, we speculate that Tet2 is involved in the regulation of senescence-related processes in $CD4^+$ T cells.

Discussion

Psoriasis is an inflammatory skin disease with a relapsing-remitting course. As mentioned above,, many traditional medicines may entail unforeseen side effects, whereas generate unexpected side effects, while highly effective biological agents are expensive [4, 6]. In addition, some patients exhibit poor responsiveness to these existing drugs [1, 4]. Thus, further studies on the pathogenesis and treatment are needed. Our findings revealed an increase in the percentage of senescent $CD4^+$ T cells and the levels of the antiapoptotic proteins BCL-2 and BCL-xL in psoriatic lesions. Thus, we developed new formulations for a BCL-2 inhibitor, ABT-737, which has been reported to effectively eliminate senescent cells via intraperitoneal injection. Notably, both the subcutaneous injection and gel formulations of ABT-737 demonstrated efficacy in ameliorating IMQ-induced psoriasis-like lesions.

Cellular senescence is related to the pathogenesis of various autoimmune and inflammatory disorders [11, 19-24]. Previous studies have indicated incresed $p16^{INK4a}$ and p21 expression in keratinocytes of psoriatic lesions compared to nonlesional areas and normal skin [40]. Besides, elevated numbers of terminally differentiated and senescent $CD8^+$ T cells were observed in peripheral blood of psoriasis patients [41]. However, limited evidence exists regarding senescent $CD4^+$ T cells in psoriasis. Herein, we found that the proportions of dermal $CD4^+$ $p16^{INK4a+}$ and $CD4^+$ $p21^+$ T cells were significantly greater in human psoriatic lesions than in controls. Moreover, BCL-2 and BCL-xL expression was upregulated in psoriatic lesions, consistent with previous studies showing increased expression of BCL-2 family members in senescent cells [19]. In addition, topical application of ABT-737 gel

demonstrated the potential to eliminate cellular senescence, thereby ameliorating IMQ-induced psoriatic lesions.

Psoriasis is characterized as an autoimmune skin disease primarily mediated by T cells [5]. The composition of T cells in the immune system consists of approximately 95% TCRαβ-expressing cells, and 5% TCRγδ- expressing cells [42]. Both TCRαβ$^+$ T cells and TCRγδ$^+$ T cells are crucial for the pathogenesis of psoriasis, [43-45]. In human psoriasis, the majority of T cells in both affected and healthy skins are αβ T cells, and the proportion of γδ T cells is approximately 1% in active psoriasis [43]. Among the 70 most frequent putative pathogenic T cell clones are αβ T cells [43]. Notably, IL-17-producing αβ T cells are present in resolved psoriatic skin lesions and function as disease-initiating pathogenic T cells in psoriasis [43]. This evidence indicates that human psoriasis is driven by αβ T cells. Additionally, IL-17$^+$ αβ T cells serve as mediators of IMQ-induced psoriasiform dermatitis.

T cells rely on TCR activation to exert their function [31]. The specificity of antigens relies on the structural diversity of the TCR, especially the three CDRs [31]. The CDR3 of the TCR has been extensively utilized to explore the function of T cells in immune responses [31]. Unique TCRα and TCRβ CDR3 sequences were found to be shared among multiple psoriasis patients but not among HCs [43]. One study revealed that the immunological features of the TCR β chain (TRB)- CDR3 region differed between patients and HCs [30]. These findings indicated a potential pathogenic role of TCRα and TCRβ CDR3 in the development of human psoriatic lesions [30, 31, 46]. In addition, therapies that modulate TCR signaling have been shown to delay the progression of psoriasis [47]. Herein, we found that the expression of the TCR α and TCR β chains in psoriatic lesions decreased

after the topical application of ABT-737 gel to IMQ-induced psoriatic lesions, as determined by immune repertoire sequencing. This result also indicated that the percentage of adaptive immune cells related to senescent cells, such as senescent $CD4^+$ T cells, could be reduced after the application of ABT-737.

In the past several decades, studies have reported that TET2 can contribute to DNA demethylation and the activation of inflammatory factors in T cells, with a greater impact on Th17 cells than on Th1 cells [35]. In addition, the roles of TET2 and 5-hmC in cellular senescence are controversial. Some studies revealed an increase in *Tet2* expression in the cerebellum of elderly mice and HaCaT cells after UVB exposure [36, 37]. However, the expression of TET2 was also reportedly decreased in the skin of aging mice [50]. Herein, we found elevated TET2 expression in senescent $CD4^+$ T cells from patients with psoriasis, and decreased *Tet2* mRNA expression after the topical application of ABT-737 gel to IMQ-induced psoriatic lesions; furthermore, psoriatic lesions were significantly alleviated, and the percentage of senescent $CD4^+$ T cells and the frequencies of Th1 and Th17 cells among $CD4^+$ T cells were significantly lower in IMQ-induced psoriatic lesions from $CD4^{cre}Tet2^{f/f}$ mice than in those from $Tet2^{f/f}$ mice. Thus, we proposed that the ABT-737 gel downregulated the TET2 expression to eliminate senescent $CD4^+$ T cells and impaired the TET2-Th17 pathway, leading to the alleviation of skin lesions in the psoriatic model. However, given the limited abundance of senescent T cells in the skin, we investigated and validated the involvement of TET2 in psoriasis and senescence primarily through $CD4^+$ T cells, as opposed to senescent $CD4^+$ T cells. This limitation should be acknowledged. To gain a more comprehensive understanding of the roles and underlying mechanisms of TET2

in senescent T cells and psoriasis, it would be necessary to conduct a specific knockout of the TET2 gene in senescent T cells.

Acknowledgments

We thank Professor Akihiko Yoshimura for providing us with the $Tet2^{f/f}$ mice.

References

[1] A.W. Armstrong, C. Read, Pathophysiology, Clinical Presentation, and Treatment of Psoriasis: A Review, Jama 323(19) (2020) 1945-1960.
[2] M. Diani, G. Altomare, E. Reali, T cell responses in psoriasis and psoriatic arthritis, Autoimmunity reviews 14(4) (2015) 286-92.
[3] M.A. Lowes, M. Suárez-Fariñas, J.G. Krueger, Immunology of psoriasis, Annual review of immunology 32 (2014) 227-55.
[4] C. Conrad, M. Gilliet, Psoriasis: from Pathogenesis to Targeted Therapies, Clinical reviews in allergy & immunology 54(1) (2018) 102-113.
[5] A. Rendon, K. Schäkel, Psoriasis Pathogenesis and Treatment, International journal of molecular sciences 20(6) (2019).
[6] N.E. Natsis, J.F. Merola, J.M. Weinberg, J.J. Wu, A.M. Orbai, J. Bagel, A.B. Gottlieb, Treatment of Medicare Patients with Moderate-to-Severe Psoriasis who Cannot Afford Biologics or Apremilast, Am J Clin Dermatol 21(1) (2020) 109-117.
[7] R.G. Langley, G.G. Krueger, C.E. Griffiths, Psoriasis: epidemiology, clinical features, and quality of life, Annals of the rheumatic diseases 64 Suppl 2(Suppl 2) (2005) ii18-23; discussion ii24-5.
[8] A. Kvist-Hansen, P.R. Hansen, L. Skov, Systemic Treatment of Psoriasis with JAK Inhibitors: A Review, Dermatology and therapy 10(1) (2020) 29-42.
[9] J. Campisi, F. d'Adda di Fagagna, Cellular senescence: when bad things happen to good cells, Nature reviews. Molecular cell biology 8(9) (2007) 729-40.
[10] S. Khosla, J.N. Farr, T. Tchkonia, J.L. Kirkland, The role of cellular senescence in ageing and endocrine disease, Nature reviews. Endocrinology 16(5) (2020) 263-275.
[11] S. He, N.E. Sharpless, Senescence in Health and Disease, Cell 169(6) (2017) 1000-1011.
[12] C.M. Adams, S. Clark-Garvey, P. Porcu, C.M. Eischen, Targeting the Bcl-2 Family in B Cell Lymphoma, Frontiers in oncology 8 (2018) 636.
[13] N. Martin, N. Popgeorgiev, G. Ichim, D. Bernard, BCL-2 proteins in senescence: beyond a simple target for senolysis?, Nature reviews. Molecular cell biology 24(8) (2023) 517-518.
[14] D. Barriuso, L. Alvarez-Frutos, L. Gonzalez-Gutierrez, O. Motiño, G. Kroemer, R. Palacios-Ramirez, L. Senovilla, Involvement of Bcl-2 Family Proteins in Tetraploidization-Related Senescence, International journal of molecular sciences 24(7) (2023).
[15] B. Tombor, K. Rundell, Z.N. Oltvai, Bcl-2 promotes premature senescence induced by oncogenic Ras, Biochemical and biophysical research communications 303(3) (2003) 800-7.
[16] A. Basu, The interplay between apoptosis and cellular senescence: Bcl-2 family proteins as targets for cancer therapy, Pharmacology & therapeutics 230 (2022) 107943.
[17] B.G. Childs, M. Durik, D.J. Baker, J.M. van Deursen, Cellular senescence in aging and age-related disease: from mechanisms to therapy, Nature medicine 21(12) (2015) 1424-35.
[18] A. Ashkenazi, W.J. Fairbrother, J.D. Leverson, A.J. Souers, From basic apoptosis discoveries to advanced selective BCL-2 family inhibitors, Nature reviews. Drug discovery 16(4) (2017) 273-284.
[19] R. Yosef, N. Pilpel, R. Tokarsky-Amiel, A. Biran, Y. Ovadya, S. Cohen, E. Vadai, L. Dassa, E. Shahar, R. Condiotti, I. Ben-Porath, V. Krizhanovsky, Directed elimination of senescent cells by inhibition of BCL-W and BCL-XL, Nature communications 7 (2016) 11190.
[20] S. Crespo-Garcia, P.R. Tsuruda, A. Dejda, R.D. Ryan, F. Fournier, S.Y. Chaney, F. Pilon, T. Dogan, G. Cagnone, P. Patel, M. Buscarlet, S. Dasgupta, G. Girouard, S.R. Rao, A.M. Wilson, R. O'Brien, R. Juneau, V. Guber, A. Dubrac, C. Beausejour, S. Armstrong, F.A. Mallette, C.B. Yohn, J.S. Joyal, D. Marquess, P.J. Beltran, P. Sapieha, Pathological angiogenesis in retinopathy engages cellular senescence and is amenable to therapeutic elimination via BCL-xL inhibition, Cell metabolism 33(4) (2021) 818-832.e7.
[21] B. Ritschka, T. Knauer-Meyer, D.S. Gonçalves, A. Mas, J.L. Plassat, M. Durik, H. Jacobs, E. Pedone, U. Di Vicino, M.P. Cosma, W.M. Keyes, The senotherapeutic drug ABT-737 disrupts aberrant p21 expression to restore liver regeneration in adult mice, Genes & development 34(7-8) (2020) 489-494.
[22] P.J. Thompson, A. Shah, V. Ntranos, F. Van Gool, M. Atkinson, A. Bhushan, Targeted Elimination of Senescent Beta Cells Prevents Type 1 Diabetes, Cell metabolism 29(5) (2019) 1045-1060.e10.

[23] C. Aguayo-Mazzucato, J. Andle, T.B. Lee, Jr., A. Midha, L. Talemal, V. Chipashvili, J. Hollister-Lock, J. van Deursen, G. Weir, S. Bonner-Weir, Acceleration of β Cell Aging Determines Diabetes and Senolysis Improves Disease Outcomes, Cell metabolism 30(1) (2019) 129-142.e4.
[24] J. Pan, D. Li, Y. Xu, J. Zhang, Y. Wang, M. Chen, S. Lin, L. Huang, E.J. Chung, D.E. Citrin, Y. Wang, M. Hauer-Jensen, D. Zhou, A. Meng, Inhibition of Bcl-2/xl With ABT-263 Selectively Kills Senescent Type II Pneumocytes and Reverses Persistent Pulmonary Fibrosis Induced by Ionizing Radiation in Mice, Int J Radiat Oncol Biol Phys 99(2) (2017) 353-361.
[25] G. Vlahovic, V. Karantza, D. Wang, D. Cosgrove, N. Rudersdorf, J. Yang, H. Xiong, T. Busman, M. Mabry, A phase I safety and pharmacokinetic study of ABT-263 in combination with carboplatin/paclitaxel in the treatment of patients with solid tumors, Investigational new drugs 32(5) (2014) 976-84.
[26] P.J. Rochette, D.E. Brash, Progressive apoptosis resistance prior to senescence and control by the anti-apoptotic protein BCL-xL, Mechanisms of ageing and development 129(4) (2008) 207-14.
[27] L. van der Fits, S. Mourits, J.S. Voerman, M. Kant, L. Boon, J.D. Laman, F. Cornelissen, A.M. Mus, E. Florencia, E.P. Prens, E. Lubberts, Imiquimod-induced psoriasis-like skin inflammation in mice is mediated via the IL-23/IL-17 axis, Journal of immunology (Baltimore, Md. : 1950) 182(9) (2009) 5836-45.
[28] P. Marrack, J. Kappler, The T cell receptor, Science (New York, N.Y.) 238(4830) (1987) 1073-9.
[29] S. Friedensohn, T.A. Khan, S.T. Reddy, Advanced Methodologies in High-Throughput Sequencing of Immune Repertoires, Trends in biotechnology 35(3) (2017) 203-214.
[30] X. Cao, Q. Wa, Q. Wang, L. Li, X. Liu, L. An, R. Cai, M. Du, Y. Qiu, J. Han, C. Wang, X. Wang, C. Guo, Y. Lu, X. Ma, High throughput sequencing reveals the diversity of TRB-CDR3 repertoire in patients with psoriasis vulgaris, International immunopharmacology 40 (2016) 487-491.
[31] H.Y. Hwang, T.G. Kim, T.Y. Kim, Analysis of T cell receptor alpha-chain variable region (Valpha) usage and CDR3alpha of T cells infiltrated into lesions of psoriasis patients, Molecular immunology 43(5) (2006) 420-5.
[32] T. Oltersdorf, S.W. Elmore, A.R. Shoemaker, R.C. Armstrong, D.J. Augeri, B.A. Belli, M. Bruncko, T.L. Deckwerth, J. Dinges, P.J. Hajduk, M.K. Joseph, S. Kitada, S.J. Korsmeyer, A.R. Kunzer, A. Letai, C. Li, M.J. Mitten, D.G. Nettesheim, S. Ng, P.M. Nimmer, J.M. O'Connor, A. Oleksijew, A.M. Petros, J.C. Reed, W. Shen, S.K. Tahir, C.B. Thompson, K.J. Tomaselli, B. Wang, M.D. Wendt, H. Zhang, S.W. Fesik, S.H. Rosenberg, An inhibitor of Bcl-2 family proteins induces regression of solid tumours, Nature 435(7042) (2005) 677-81.
[33] M. Konopleva, R. Contractor, T. Tsao, I. Samudio, P.P. Ruvolo, S. Kitada, X. Deng, D. Zhai, Y.X. Shi, T. Sneed, M. Verhaegen, M. Soengas, V.R. Ruvolo, T. McQueen, W.D. Schober, J.C. Watt, T. Jiffar, X. Ling, F.C. Marini, D. Harris, M. Dietrich, Z. Estrov, J. McCubrey, W.S. May, J.C. Reed, M. Andreeff, Mechanisms of apoptosis sensitivity and resistance to the BH3 mimetic ABT-737 in acute myeloid leukemia, Cancer cell 10(5) (2006) 375-88.
[34] R. Mazzone, C. Zwergel, M. Artico, S. Taurone, M. Ralli, A. Greco, A. Mai, The emerging role of epigenetics in human autoimmune disorders, Clinical epigenetics 11(1) (2019) 34.
[35] K. Ichiyama, T. Chen, X. Wang, X. Yan, B.S. Kim, S. Tanaka, D. Ndiaye-Lobry, Y. Deng, Y. Zou, P. Zheng, Q. Tian, I. Aifantis, L. Wei, C. Dong, The methylcytosine dioxygenase Tet2 promotes DNA demethylation and activation of cytokine gene expression in T cells, Immunity 42(4) (2015) 613-26.
[36] D. Wang, J.H. Huang, Q.H. Zeng, C. Gu, S. Ding, J.Y. Lu, J. Chen, S.B. Yang, Increased 5-hydroxymethylcytosine and Ten-eleven Translocation Protein Expression in Ultraviolet B-irradiated HaCaT Cells, Chinese medical journal 130(5) (2017) 594-599.
[37] S. Dzitoyeva, H. Chen, H. Manev, Effect of aging on 5-hydroxymethylcytosine in brain mitochondria, Neurobiology of aging 33(12) (2012) 2881-91.
[38] J. Jiang, M. Zhao, C. Chang, H. Wu, Q. Lu, Type I Interferons in the Pathogenesis and Treatment of Autoimmune Diseases, Clinical reviews in allergy & immunology 59(2) (2020) 248-272.
[39] T. Torres, P. Filipe, Small Molecules in the Treatment of Psoriasis, Drug development research 76(5) (2015) 215-27.
[40] L. Mercurio, D. Lulli, F. Mascia, E. Dellambra, C. Scarponi, M. Morelli, C. Valente, M.L. Carbone, S. Pallotta, G. Girolomoni, C. Albanesi, S. Pastore, S. Madonna, Intracellular Insulin-like growth factor binding protein 2 (IGFBP2) contributes to the senescence of keratinocytes in psoriasis by stabilizing cytoplasmic p21, Aging 12(8) (2020) 6823-6851.
[41] L. Sahmatova, E. Sugis, M. Sunina, H. Hermann, E. Prans, M. Pihlap, K. Abram, A. Rebane, H. Peterson, P. Peterson, K. Kingo, K. Kisand, Signs of innate immune activation and premature immunosenescence in psoriasis patients, Sci Rep 7(1) (2017) 7553.
[42] D. Brandt, C.M. Hedrich, TCRαβ(+)CD3(+)CD4(-)CD8(-) (double negative) T cells in autoimmunity, Autoimmunity reviews 17(4) (2018) 422-430.

[43] T.R. Matos, J.T. O'Malley, E.L. Lowry, D. Hamm, I.R. Kirsch, H.S. Robins, T.S. Kupper, J.G. Krueger, R.A. Clark, Clinically resolved psoriatic lesions contain psoriasis-specific IL-17-producing αβ T cell clones, The Journal of clinical investigation 127(11) (2017) 4031-4041.
[44] T. Nomura, K. Kabashima, Y. Miyachi, The panoply of αβT cells in the skin, Journal of dermatological science 76(1) (2014) 3-9.
[45] S. Nishimoto, H. Kotani, S. Tsuruta, N. Shimizu, M. Ito, T. Shichita, R. Morita, H. Takahashi, M. Amagai, A. Yoshimura, Th17 cells carrying TCR recognizing epidermal autoantigen induce psoriasis-like skin inflammation, Journal of immunology (Baltimore, Md. : 1950) 191(6) (2013) 3065-72.
[46] L. Diluvio, S. Vollmer, P. Besgen, J.W. Ellwart, S. Chimenti, J.C. Prinz, Identical TCR beta-chain rearrangements in streptococcal angina and skin lesions of patients with psoriasis vulgaris, Journal of immunology (Baltimore, Md. : 1950) 176(11) (2006) 7104-11.
[47] A. Borroto, D. Reyes-Garau, M.A. Jiménez, E. Carrasco, B. Moreno, S. Martínez-Pasamar, J.R. Cortés, A. Perona, D. Abia, S. Blanco, M. Fuentes, I. Arellano, J. Lobo, H. Heidarieh, J. Rueda, P. Esteve, D. Cibrián, A. Martinez-Riaño, P. Mendoza, C. Prieto, E. Calleja, C.L. Oeste, A. Orfao, M. Fresno, F. Sánchez-Madrid, A. Alcamí, P. Bovolenta, P. Martín, P. Villoslada, A. Morreale, A. Messeguer, B. Alarcon, First-in-class inhibitor of the T cell receptor for the treatment of autoimmune diseases, Science translational medicine 8(370) (2016) 370ra184.
[48] X. Wang, X. Liu, X. Duan, K. Zhu, S. Zhang, L. Gan, N. Liu, H. Jaypaul, J.T. Makamure, Z. Ming, H. Chen, Ten-eleven Translocation-2 Regulates DNA Hydroxymethylation Status and Psoriasiform Dermatitis Progression in Mice, Acta Derm Venereol 98(6) (2018) 585-593.
[49] X. Wang, X. Liu, N. Liu, H. Chen, Prediction of crucial epigenetically-associated, differentially expressed genes by integrated bioinformatics analysis and the identification of S100A9 as a novel biomarker in psoriasis, International journal of molecular medicine 45(1) (2020) 93-102.
[50] H. Qian, X. Xu, Reduction in DNA methyltransferases and alteration of DNA methylation pattern associate with mouse skin ageing, Exp Dermatol 23(5) (2014) 357-9.

Legends

Figure 1. Increased percentages of $CD4^+$ $p16^{INK4a+}$ and $CD4^+$ $p21^+$ T cells in human psoriatic lesions.

Figure 2. Subcutaneous injection of ABT-737 and topical application of ABT-737 gel ameliorated IMQ-induced psoriasis-like lesions.

Figure 3. Topical application of ABT-737 gel significantly reduced the frequency of senescent $CD4^+$ T cells and decreased the mRNA expression levels of inflammatory cytokines and SASPs in IMQ-induced psoriasis-like lesions.

Figure 4. Topical application of ABT-737 gel decreased the expression of TCR α and β chains in IMQ-induced psoriatic lesions, as determined via immune repertoire sequencing.

Figure 5. No systemic effects were observed in the IMQ-induced psoriasis-like mouse model following treatment with the ABT-737 gel.

Figure 6. Topical application of ABT-737 gel reduced the expression of TET2, and the absence of TET2 in $CD4^+$ T cells alleviated IMQ-induced psoriatic lesions, as indicated by decreased numbers of senescent $CD4^+$ T cells and reduced percentages of Th1 and Th17 cells.

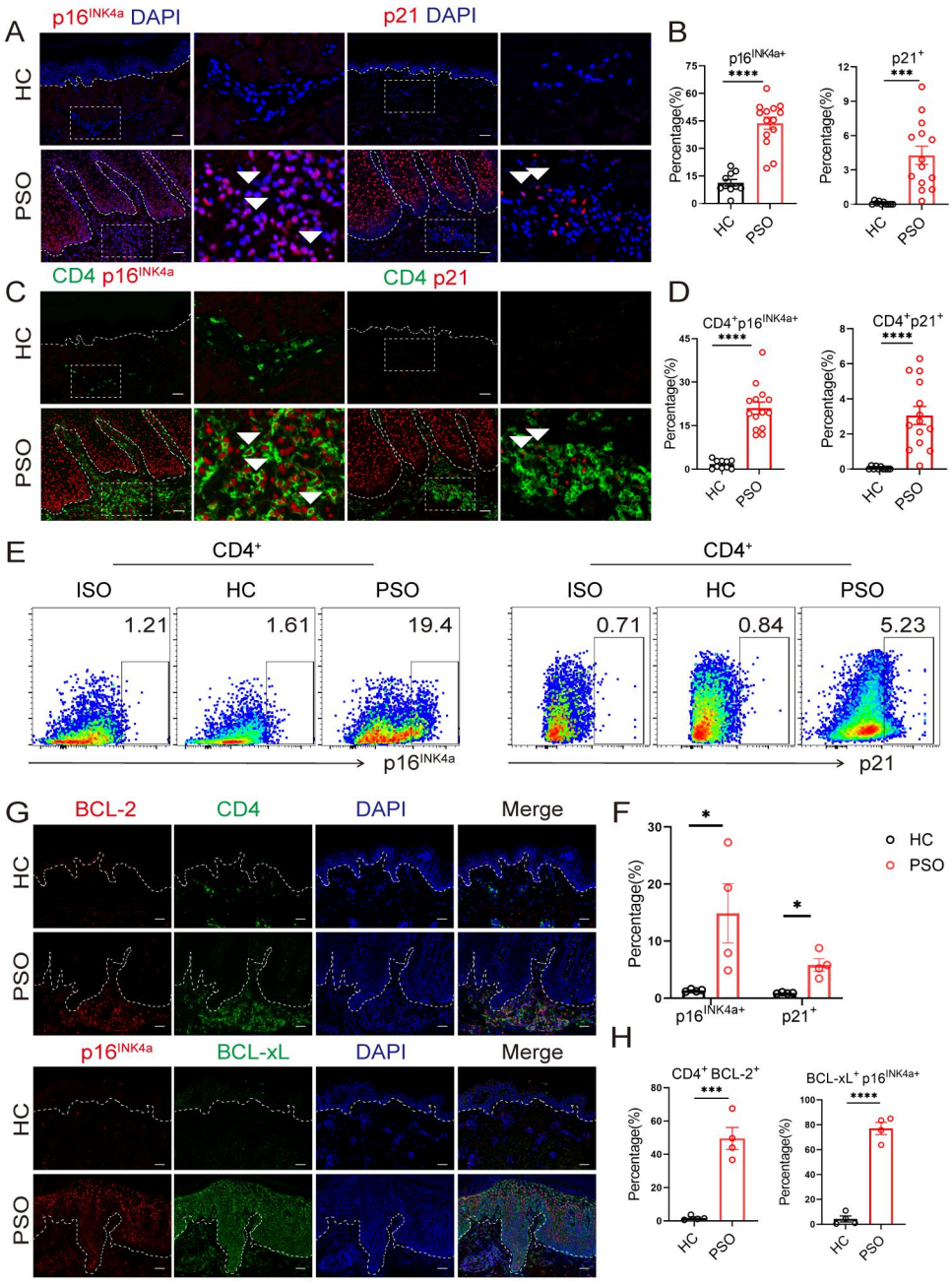

Figure 1. Increased percentages of CD4$^+$ p16^{INK4a+} and CD4$^+$ p21$^+$ T cells in human psoriatic lesions. (A) mIHC staining of p16^{INK4a} (red) or p21 (red) along with DAPI (blue) in psoriatic skin lesions and HC samples. (B) Statistical analysis of the frequencies of p16^{INK4a+} and p21$^+$ cells within dermal cells of skin samples from HCs (n=10) and psoriasis patients (n=14). (C) mIHC staining of CD4 (green) with p16^{INK4a} (red) or CD4 (green) with p21 (red) in skin samples

from HCs and patients with psoriasis. (D) Statistical analysis of the frequencies of $CD4^+$ $p16^{INK4a+}$ and $CD4^+$ $p21^+$ T cells within dermal cells of skin samples from HCs (n=10) and patients with psoriasis (n=14). (E-F) Representative flow cytometry diagrams and statistical analysis of the frequencies of $p16^{INK4a+}$ cells or $p21^+$ cells in the skin $CD4^+$ T cells of psoriasis (n=4) and HCs (n=4). (G) mIHC staining of CD4 (green) with BCL-2 (red) or BCL-xL (green) with $p16^{INK4a+}$ (red) in skin samples from HCs and patients with psoriasis. (H) Statistical analysis of the percentages of $CD4^+BCL\text{-}2^+$ and $BCL\text{-}xL^+p16^{INK4a+}$ cells within skin samples from HCs (n=4) and psoriatic patients (n=4). Data are representative of a semiquantitative analysis of the mean absorbance (Am) and integral absorbance (Ai) of at least 5 random sites in each sample. White scale represents 50um.

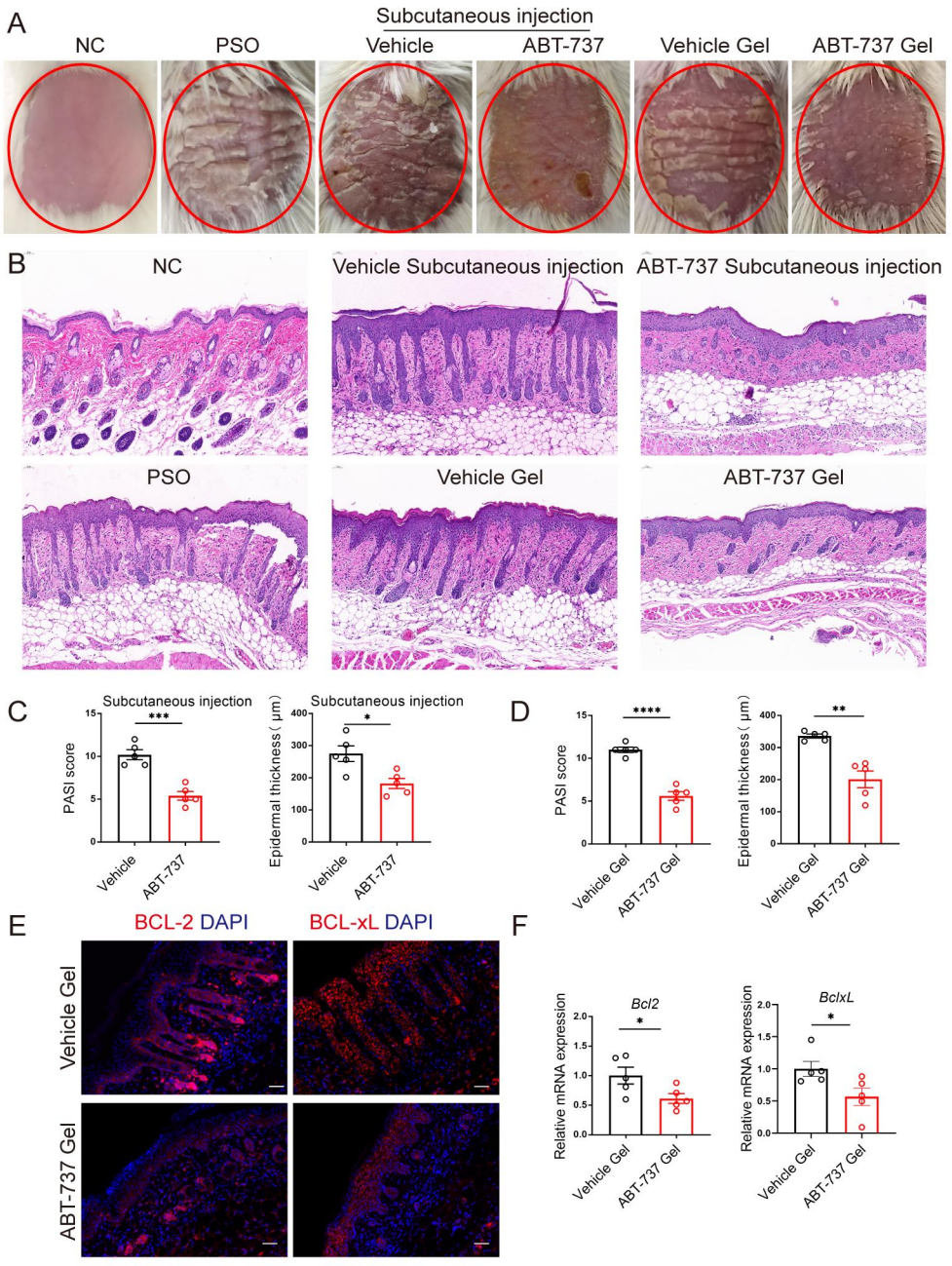

Figure 2. Subcutaneous injection of ABT-737 and topical application of ABT-737 gel ameliorated IMQ-induced psoriasis-like lesions. (A-B) Representative images of the clinical appearance of the skin (A) and H&E-stained skin (B) on the shaved back of the IMQ-induced psoriasis-like mouse model after treatment with different interventions. (C) Statistical analysis of the PASI scores and epidermal thickness in IMQ-induced psoriasis-like mice following

subcutaneous injections of ABT-737 (n=5) or an equivalent vehicle (n=5). (D) Statistical analysis of the PASI scores and epidermal thickness in IMQ-induced psoriasis-like mice following ABT-737 gel (n=5) or an equivalent vehicle gel (n=5). (E) The mIHC staining of BCL-2 (red) with DAPI (blue) or BCL-xL (red) with DAPI (blue) in skin lesions from IMQ-induced psoriasis-like mice following the ABT-737 gel (n=5) or an equivalent vehicle gel (n=5) treatment. (F) Statistical analysis of the relative mRNA expression levels of *Bcl2* and *BclxL* in IMQ-induced psoriatic lesions treated with ABT-737 gel (n=5) or an equivalent vehicle gel (n=5).

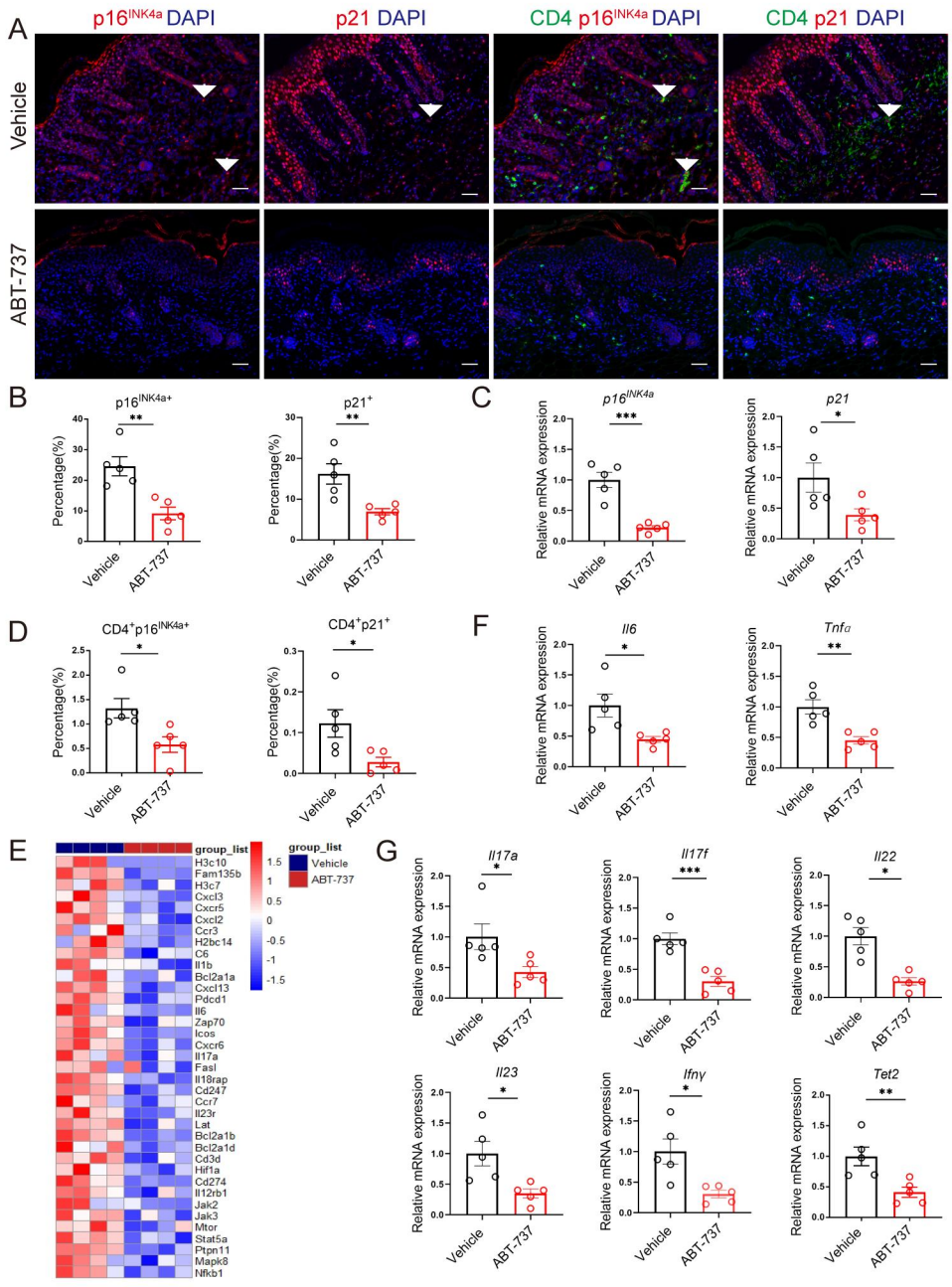

Figure 3. Topical application of ABT-737 gel significantly reduced the frequency of senescent CD4$^+$ T cells and decreased the mRNA expression levels of inflammatory cytokines and SASPs in IMQ-induced psoriasis-like lesions. (A) mIHC staining of p16^{INK4a} (red) with CD4 (green) or p21 (red) with CD4 (green) in skin lesions from an IMQ-induced psoriatic model treated with ABT-737 gel (n=5) or vehicle gel (n=5). (B) Statistical analysis of

the frequencies of $p16^{INK4a+}$ and $p21^{+}$ cells in IMQ-induced psoriatic lesions after treatment with the ABT-737 gel (n=5) or vehicle gel (n=5). (C) Statistical analysis of the relative mRNA expression levels of *p16*^{INK4a} and *p21* in IMQ-induced psoriatic lesions treated with the ABT-737 gel (n=5) or equivalent vehicle gel (n=5). (D) Statistical analysis of the frequencies of $CD4^{+}$ $p16^{INK4a+}$ and $CD4^{+}$ $p21^{+}$ T cells in IMQ-induced psoriatic lesions after treatment with the ABT-737 gel (n=5) or vehicle gel (n=5). (E) Clustered heatmap of 37 signature genes in IMQ-induced psoriatic lesions after treatment with the ABT-737 gel (n=4) or vehicle gel (n=4). (F-G) Statistical analysis of the relative mRNA expression levels of *Il17a*, *Il17f*, *Il22*, *Il23*, *Ifnγ, Il6, Tnfα* and *Tet2* in IMQ-induced psoriatic lesions treated with ABT-737 gel (n=5) or an equivalent vehicle gel (n=5).

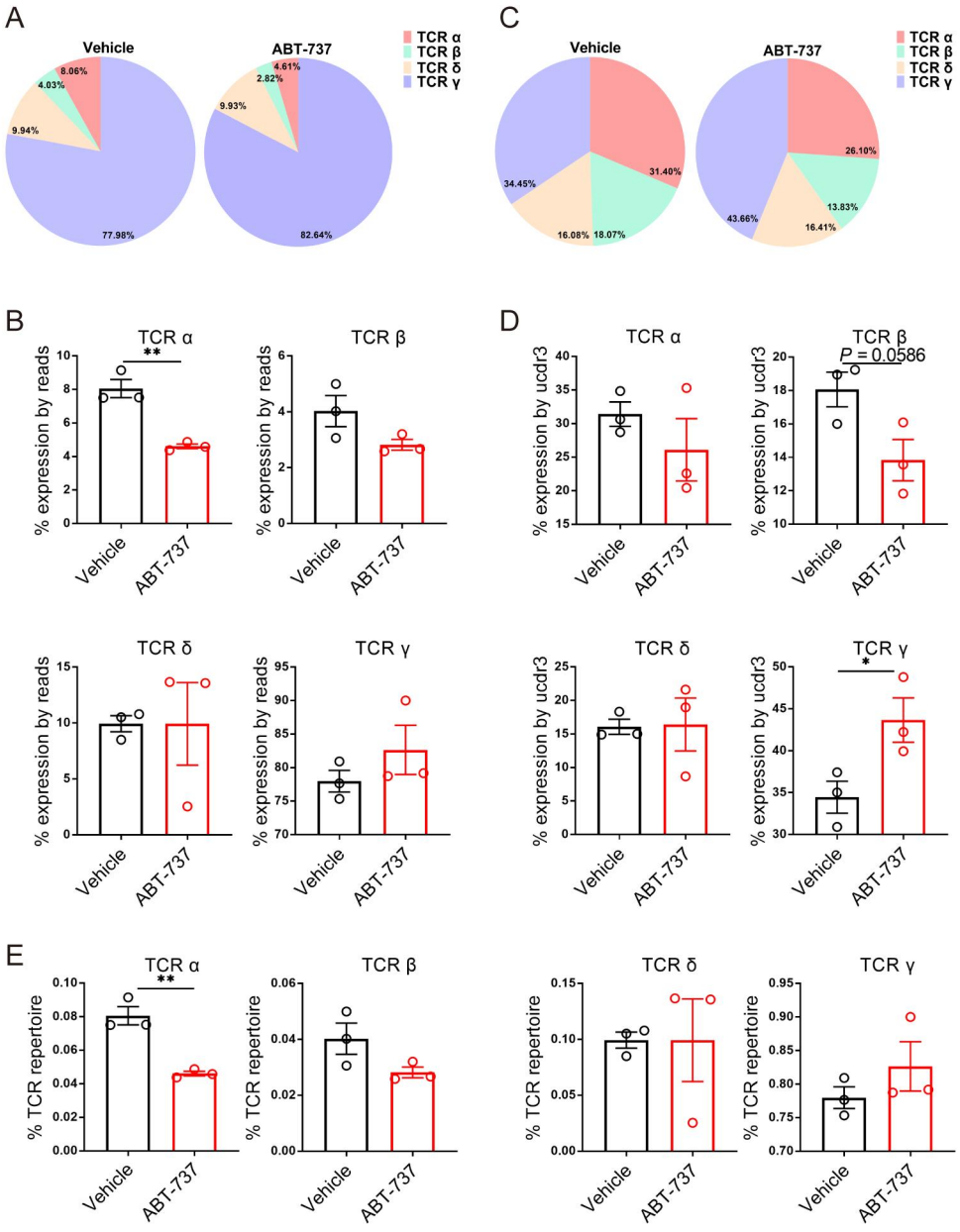

Figure 4. Topical application of ABT-737 gel decreased the expression of TCR α and β chains in IMQ-induced psoriatic lesions, as determined via immune repertoire sequencing. (A-B) Analysis of the percentages of the expression of 4 TCR chains, as determined by reads, in IMQ-induced psoriatic lesions treated with the ABT-737 gel (n=3) or vehicle gel (n=3) via immune repertoire sequencing. Data are representative and are presented as the mean values. (C-

D) Analysis of the percentages of 4 TCR chains, as determined by uCDR3, in IMQ-induced psoriatic lesions treated with the ABT-737 gel (n=3) or vehicle gel (n=3) using the immune repertoire sequencing. Data are representative and are presented as the mean values. (E) Statistical analysis of the percentages of 4 TCR chains in T cells of the 4 TCR chains in IMQ-induced psoriatic lesions treated with the ABT-737 gel (n=3) or vehicle gel (n=3). Data are representative and are presented as the mean values.

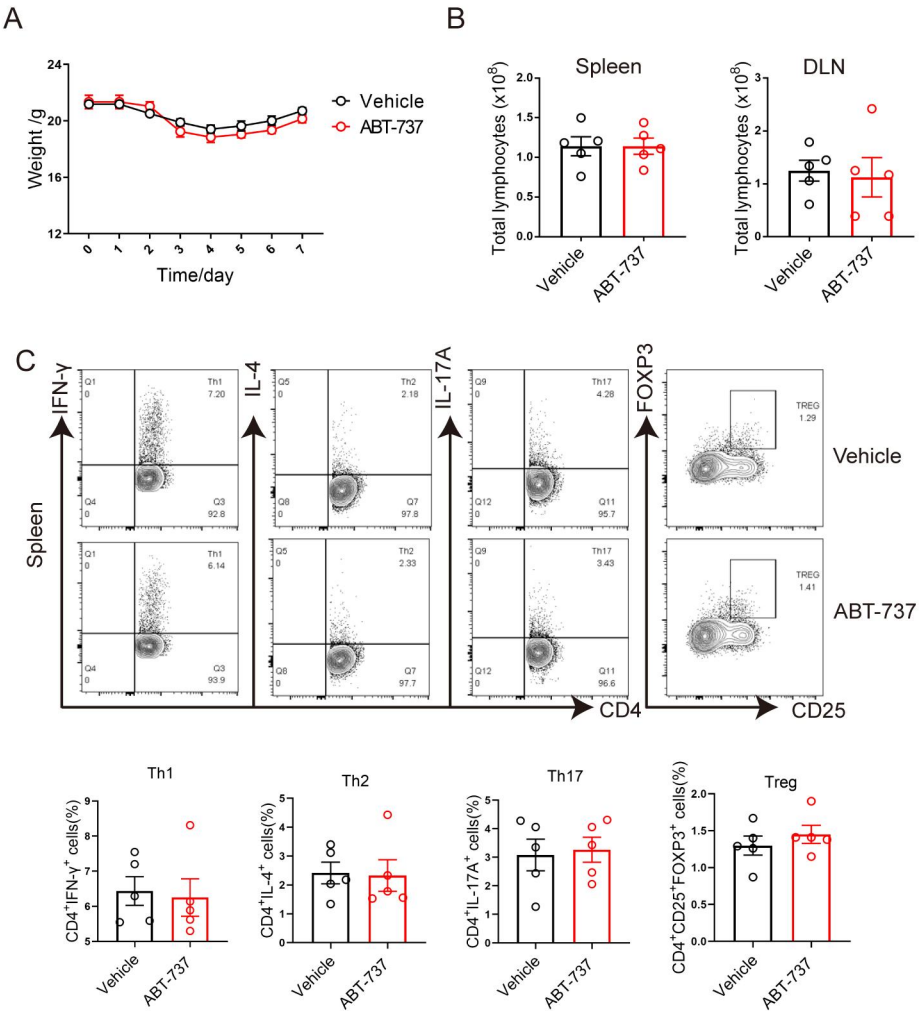

Figure 5. No systemic effects were observed in the IMQ-induced psoriasis-like mouse model following treatment with the ABT-737 gel. (A) Analysis of the weights of IMQ-induced psoriatic mice treated with the ABT-737 gel (n=5) or vehicle gel (n=5). (B) Total number of lymphocyte count analysis in the spleen and DLNs (n=5). (C) Representative flow cytometry diagrams and statistical analysis of the frequencies of Th1, Th2, Th17 and Treg cells in total $CD4^+$ T cells from the spleens of IMQ-induced psoriatic mice treated with the ABT-737 gel (n=5) or vehicle gel (n=5).

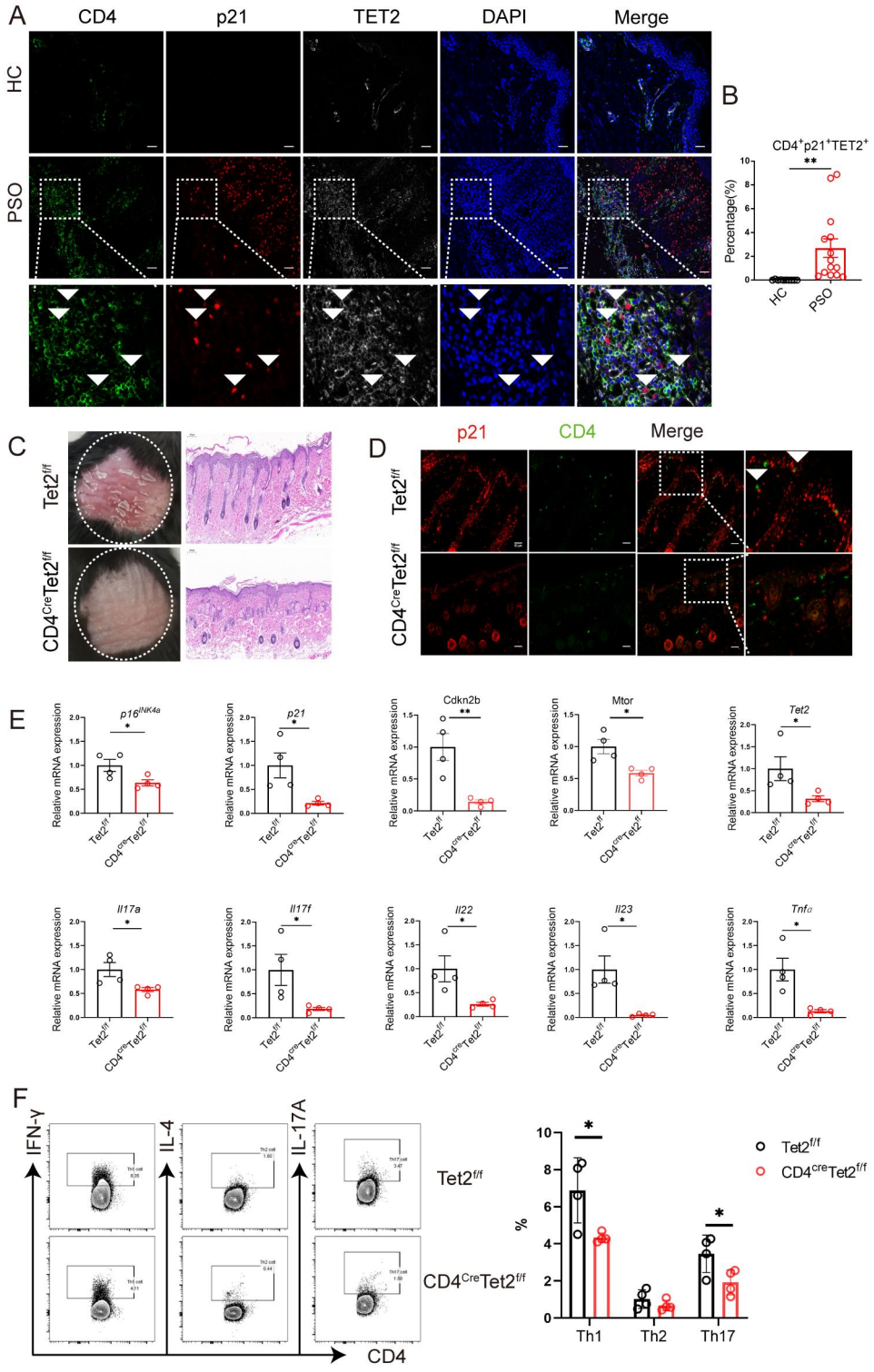
A
CD4
p21
TET2
DAPI
Merge
HC
PSO
B
CD4+p21+TET2+
Percentage(%)
HC
PSO
C
Tet2f/f
CD4CreTet2f/f
D
p21
CD4
Merge
Tet2f/f
CD4CreTet2f/f
E
p16INK4a
p21
Cdkn2b
Mtor
Tet2
Il17a
Il17f
Il22
Il23
Tnfα
Relative mRNA expression
Tet2f/f
CD4CreTet2f/f
F
IFN-γ
IL-4
IL-17A
CD4
Tet2f/f
CD4CreTet2f/f
%
Th1
Th2
Th17

Figure 6. Topical application of ABT-737 gel reduced the expression of TET2, and the absence of TET2 in $CD4^+$ T cells alleviated IMQ-induced psoriatic lesions, as indicated by decreased numbers of senescent $CD4^+$ T cells and reduced percentages of Th1 and Th17 cells. (A) Analysis of the frequency of CD4 (green), p21 (red), and TET2 (white) co-stained cells present in human psoriatic lesions by using mIHC. (B) Statistical analysis of the percentage of $CD4^+$ $p21^+$ $TET2^+$ T cells in dermal cells from skin lesions of psoriasis patients (n=14) and normal skin (n=10). (C) Representative images of the clinical appearance and H&E staining of the skin on the shaved back of IMQ-induced psoriasis-like lesions in $CD4^{cre}Tet2^{f/f}$ and $Tet2^{f/f}$ mice. (D) Analysis of the frequency of p21 (red) and CD4 (green) co-stained cells in the IMQ-induced psoriatic lesions of $CD4^{cre}Tet2^{f/f}$ and $Tet2^{f/f}$ mice by using mIHC. (E) Statistical analysis of the relative mRNA expression levels of $p16^{INK4a}$, *p21, Cdkn2b, Mtor, Tet2*, *Il17a*, *Il17f*, *Il22, Il23* and *Tnfα* in the IMQ-induced psoriatic lesions of $CD4^{cre}Tet2^{f/f}$ (n=4) and $Tet2^{f/f}$ mice (n=4). (F) Analysis of the percentages of Th1, Th2, and Th17 cells among total $CD4^+$ T cells in the spleens of IMQ-induced psoriatic $CD4^{cre}Tet2^{f/f}$ (n=4) and $Tet2^{f/f}$ mice (n=4) by using flow cytometry.

Supplementary material

Methods

1. Human subjects.

Eighteen outpatients pathologically diagnosed with plaque psoriasis and fourteen sex- and age-matched healthy volunteers were enrolled. Their detailed information is presented in Table S1A-S1B. The PASI score was used to evaluate the disease activity of psoriasis. All human subjects were recruited from the Department of Dermatology or Physical Examination Center in the Second Xiangya Hospital of Central South University. All experiments were approved by the Ethics Committee of Second Xiangya Hospital, Central South University.

2. Mice.

BALB/c mice were purchased from Slack Company. The $Tet2^{f/f}$ mice were provided by Professor Akihiko Yoshimura. We confirmed the genotypes through PCR analyses of mouse tail' genomic DNA. The primers were as follows: $CD4^{cre}$: forward 5'-GCTCGACCAGTTTAGTTACCC-3' and reverse 5'-TCGCGATTATCTTCTATATCTTCA-3'; $Tet2^{f/f}$: forward 5'-AAGAATTGCTACAGGCCTGC-3' and reverse 5'-TTCTTTAGCCCTTGCTGAGC-3'. We used 8-week-old female mice that were

maintained under specific pathogen-free conditions for all experiments.

3. IMQ-induced psoriasis-like mouse model.

In our experiment, female BALB/c, $CD4^{cre}Tet2^{f/f}$ mice, and $Tet2^{f/f}$ mice were treated with 62.5 mg of IMQ cream (5%) (Sichuan Med-shine Pharmaceutical) daily on a 2*2 cm^2 area of the shaved back for 7 days to establish the IMQ-induced psoriatic mouse model.

4. ABT-737 administration.

During the establishment of the IMQ-induced psoriasis-like mouse model, we applied a daily dose of 25 mg/kg/day ABT-737 injection, 0.5 g/day 0.05% ABT-737 gel, equivalent vehicle injection or equivalent vehicle gel on shaved backs for 7 days. The interval between the administration of the IMQ cream and the treatment was 6 hours. The ABT-737 injections were prepared using ABT-737 (ApexBio Technology), 10% DMSO (Sigma, catalog D2650), 40% PEG-300 (MCE, CAS No. 25322-68-3), 5% Tween 80 (Sigma), and 45% phosphate-buffered saline (PBS), while the vehicle injection was composed of 10% DMSO, 40% PEG-300, 5% Tween 80, and 45% PBS. For the 0.05% ABT-737 gel, the formulation was composed of ABT-737, 1% DMSO, 0.5% carbomer 940 (Meilunbio CAS No. MB1874), and purified water, while the vehicle gel was composed of 1% DMSO, 0.5% carbomer 940, and purified water.

5. Evaluation of inflammation severity in the psoriatic mouse model.

We used the PASI scoring system and evaluated erythema, scales, and thickening to determine the severity of skin inflammation [1]. Each factor was scored independently in the range of 0 to 4 points: 0, none; 1, slight; 2, moderate; 3, marked; and 4, very marked. The total PASI score was the sum of the 3 index scores (scores ranging from 0-12 points). We used CaseViewer (3DHISTECH Ltd) to measure the thickness of the epidermis. Each field of view was measured three times, and the average value was taken.

6. multi-spectrum immunohistochemistry (mIHC).

The formalin-fixed paraffin-embedded skin sections were deparaffinized, hydrated, and boiled in citrate buffer (Servicebio, cat. G1202) for antigen epitope retrieval, followed by blockade of nonspecific binding and manual incubated with primary antibodies at room temperature for 1 hour (primary antibodies including anti-human CD4 (MXB Biotechnologies, RMA-0620), anti-mouse CD4 (Abcam, cat. ab183685), anti-human CDKN2A/p16^{INK4a} (Abcam, cat. ab54210), anti-mouse CDKN2A/p16^{INK4a} (Abcam, cat. ab211542), anti-human p21 (Abcam, cat. ab109520), anti-mouse p21 (Abcam, cat. ab188224), anti-human/mouse Bcl-2 (Abcam, cat. ab182858), anti-human/mouse Bcl-xL (Abcam, cat. ab32370), and anti-human TET2 (NOVOUS, cat. NRP2-32104)). Then incubation with secondary antibody was performed at room temperature for 10 minutes (secondary antibodies including opal polymer HRP Ms+Rb (PerkinElmer, ARH1001A) for human, HRP-conjugated anti-rabbit antibody (Abcam, cat. ab205718) for mouse). Finally, the Opal 7-color IHC detection kit (PerkinElmer) was used for fluorescence

labeling. DAPI was used to visualize cell nuclei. All multispectral images in each section were captured at high magnification by the PerkinElmer Vetra multispectral imaging system (Vectra 3.0.3; PerkinElmer). The top 5 $CD4^+$ cell-infiltrating areas were analyzed, and the positive cell percentage (positive cell percentage=positive staining cells / DAPI staining cells) per high power field was measured using inForm Advanced Image Analysis software (inForm 2.3.1; PerkinElmer).

7. Flow cytometry.

We used a FACSCanto II instrument (BD Biosciences) for flow cytometry. For surface markers, we incubated cells with fluorescent antibodies on ice for 45 minutes in the dark: FITC anti-mouse CD4 (BD Biosciences, catalog 553729) and PE anti-mouse CD25 (BioLegend, catalog 102008). For transcription factors, we used a human Foxp3 buffer set (BD Biosciences) to fix and permeabilize cells, and then we incubated the samples with fluorescent antibody APC anti-mouse FOXP3 (BioLegend, catalog 2107506) on ice in the dark for 1 hour. For cytokines, we stimulated cells with PMA, ionomycin, and GolgiPlug (BD Biosciences) for 5 hours and then used Cytofix/Cytoperm buffer (BD Biosciences) for fixation as well as permeabilization. Afterwards, we stained samples with fluorescent dye-conjugated antibodies on ice in the dark for 0.5 hours: APC anti-mouse IFN-γ (BioLegend, catalog 505814), PE anti-mouse IL-4 (eBioscience, catalog 4314798), and PE/Cyanine7 anti-mouse IL-17A (BioLegend, catalog 506922).

For skin flow cytometry, the skin single-cell suspension of psoriasis and healthy controls was prepared as described [2]. For surface markers, cells were labeled with PerCP/Cyanine5.5 anti-human CD4 (BioLegend, catalog 300530) and Zombie NIR™ (BioLegend, catalog 423106) on ice in the dark for 45 minutes. The cells were then fixed and permeabilized followed by antibody anti-CDKN2A/p16INK4a (Abcam, ab108349) or anti-p21(Abcam, ab109520) for 30 minutes at 22°C. The isotype control antibody was recombinant rabbit monoclonal IgG (Abcam, ab172730). The secondary antibody goat anti-rabbit IgG H&L (Alexa Fluor® 488) (Abcam, ab150081) was incubated at 1/4000 for 30 minutes at 22°C. FlowJo software (Tree Star) was used for event collection and analysis.

8. RT-qPCR.

We used TRIzol reagent (Invitrogen) to extract total RNA from cells or skin samples and a NanoDrop spectrophotometer (ND-2000, Thermo Fisher Scientific) for RNA quality control. We used the PrimeScript RT Reagent Kit with gDNA Eraser (TaKaRa Biotech Co.) for mRNA reverse transcription, and 1 μg of total RNA was used following the manufacturer's instructions. qPCR was conducted with SYBR Premix Ex Taq II (Tli RNaseH Plus) (TaKaRa Biotech Co.) with a LightCycler 96 (Bio-Rad) thermocycler. We used the internal control *RPLP0* or *GAPDH* [3] to calculate the relative expression level. The fold change in gene expression was assessed via the formula $2^{-(\Delta Ct\ \text{experimental group} - \Delta Ct\ \text{control group})}$, which was normalized to controls. The sequences of the primers used are

shown in Table S2A-S2B.

9. RNA sequencing and bioinformatics analysis.

We extracted total RNA from IMQ-induced psoriatic lesions treated with the ABT-737 gel or vehicle gel using TRIzol reagent. RNA library preparation and sequencing were performed by BGI Genomics, China. The libraries were constructed as described in previous studies[4]. The adapter sequences as well as low-quality reads were removed by Trimmomatic v0.33 in PE FASTQ files[4]. The HTseq v0.6.0 (htseq-count) counting exon features and reporting Ensembl Gene IDs were processed to acquire annotation and gene counts[4]. Data normalization and differential expression analysis were conducted by limma voom function v3.32.10 in R v3.4.1[4].

10. Immune Repertoire Sequencing.

We amplified the total RNA from IMQ-induced psoriasis-like lesions treated with ABT-737 gel or vehicle gel and allowed the incorporation of unique molecular identifiers during the reverse transcription step by iR-RepSeq-plus-MBIvc-abdg Cassette (iRepertoire Inc, US) covering the 4 mouse TCR chains. These steps were processed as follows: sample library preparation (mouse TCR libraries), including SPRIselect bead selection (Beckman Coulter), and binding and extension with the V-gene primer mix.

Amplified libraries were multiplexed and pooled for sequencing on the Illumina MiSeq

platform using one 600-cycle kit and sequenced as 250 paired-end reads. The output of the immune receptor sequence covers the second framework region through the beginning of the constant region containing CDR2 as well as CDR3. We analyzed the raw sequencing data via the iRmap program[5].

11. ATAC sequencing

$CD4^+$ T cells were isolated from the peripheral blood of health volunteers by magnetic beads (Miltenyi). 2×10^6 cells were resuspended in 100 μL electroporation liquid, mixed with 2.5 μL TET2 siRNA (Ruibo, 20 μM), and then transfected following the human $CD4^+$ T cell protocol. Next, the $CD4^+$ T cells were seeded in a CD3 pre-coating 24-well plate (BD bioscience, 2 μg/ml) stimulated with CD28 (BD bioscience, 1 μg/ml). ABT-737 (10 μM) was then added to the corresponding culture system. After 48 hours of stimulation, fifty thousand $CD4^+$ T cells were collected for transposase-accessible-chromatin sequencing analysis, following the detailed protocol described in 3D genome alterations in T cells associated with disease activity of systemic lupus erythematosus[6].

12. Statistical analysis.

We used GraphPad Prism and SPSS software for statistical analyses. Data are shown as the means ± SEMs. Statistical significance (* $p < 0.05$, ** $p < 0.01$, *** $p < 0.001$, and **** $p < 0.0001$) was compared by two-tailed unpaired Student's t test for two

independent groups. The unpaired t-test can determine whether there is a difference between two unrelated groups. When the data did not conform to a normal distribution or homogeneity of variance, the two-tailed Mann–Whitney *U* test was performed.

13. Study approval.

All animal care protocols and experiments were approved by the Ethics Committee of Second Xiangya Hospital, Central South University, and informed consent was acquired from participants for all experiments performed with human subjects after the nature and possible consequences of the studies were explained.

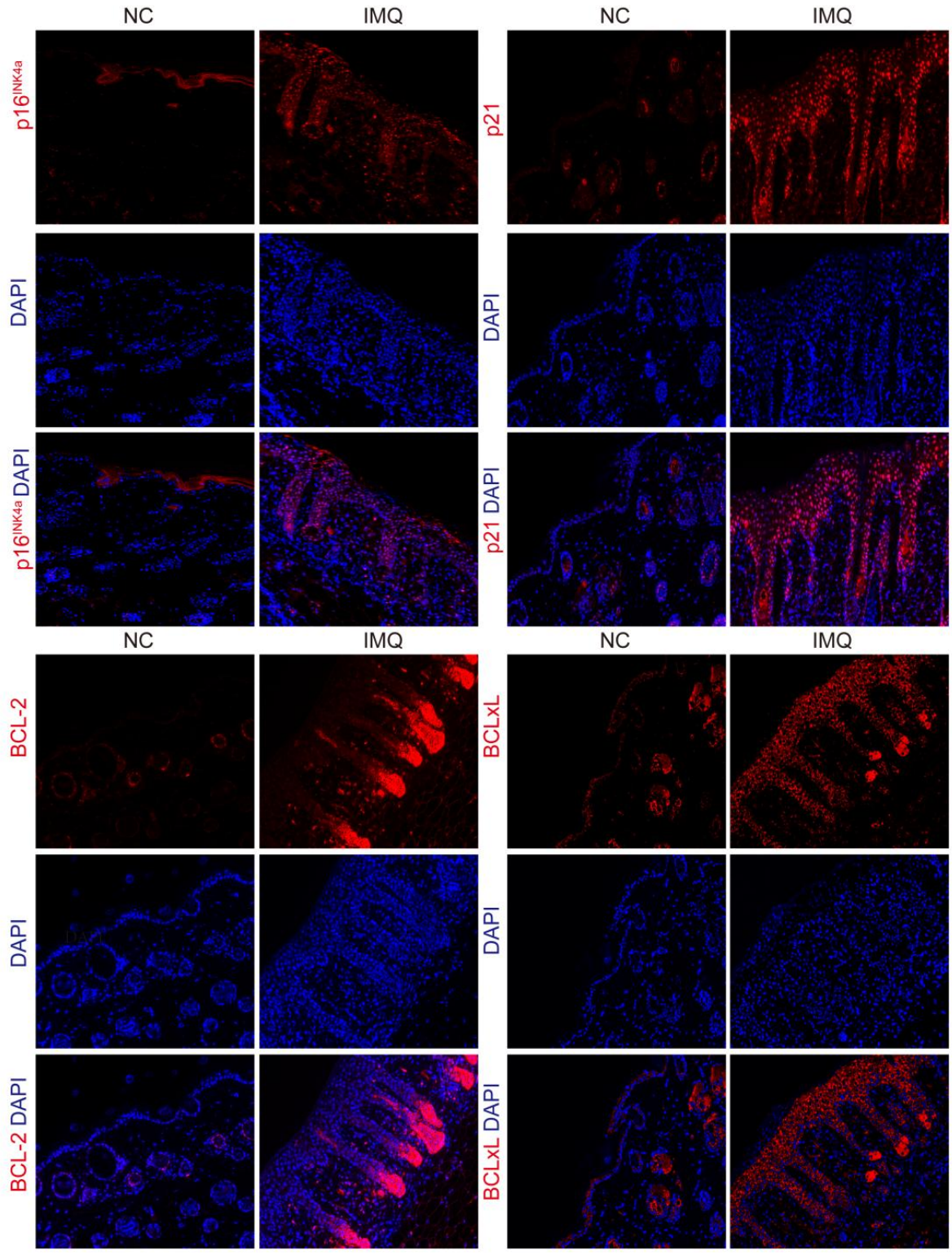

Figure S1. Increased percentage of $p16^{INK4a+}$, $p21^{+}$, BCL-2^{+} and BCL-xL^{+} cells in

IMQ-induced psoriasis-like lesions. The mIHC staining of $p^{16INK4a+}$ (red), $p21^{+}$ (red), BCL-2^{+} (red) or BCL-xL^{+} (red) and DAPI (blue) in skin lesions from IMQ-induced psoriasis-like lesions and normal skin in BALB/c mice

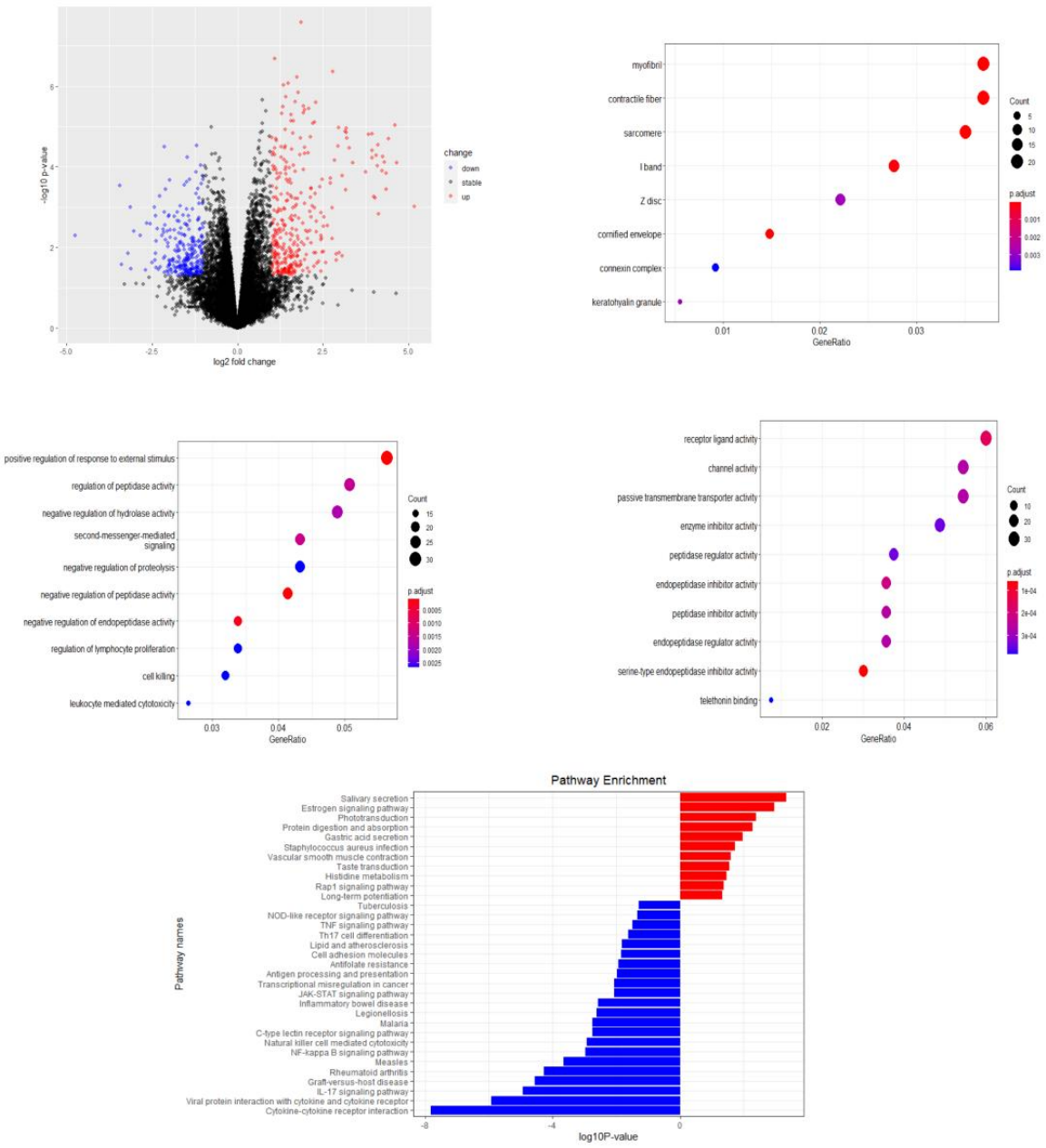

Figure S2. Information of RNA-seq in total RNA from IMQ-induced psoriasis-like lesions treated with ABT-737 gel or vehicle.

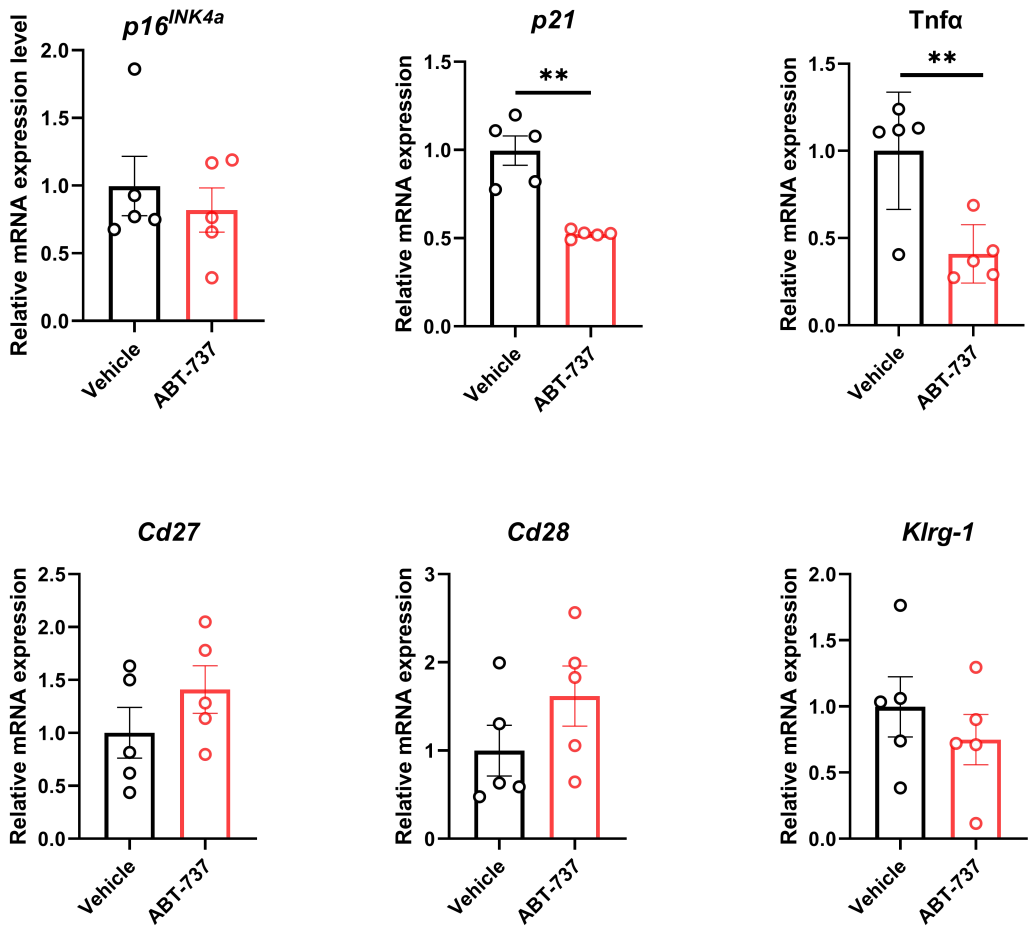

Figure S3. The effects of ABT-737 gel in the mRNA expression levels of genes related to cellular senescence in the spleen of IMQ-induced psoriasis mouse model. Statistical analysis of the relative mRNA expression levels of *p16*^{INK4a}, *p21*, *Tnfα*, *Cd27*, *Cd28* and *Klrg-1* in the spleen of the IMQ-induced psoriasis mouse model treated with ABT-737 gel (n=5) or equivalent vehicle gel (n=5).

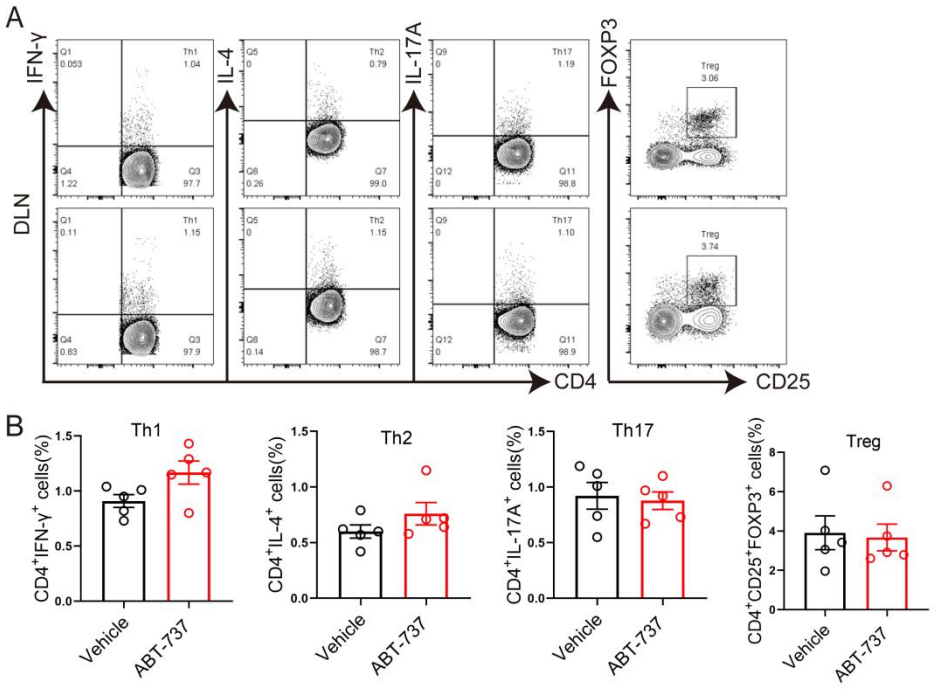

Figure S4. ABT-737 gel treatment had no effects on the percentage of Th1/Th2/Th17/Treg among CD4$^+$ T cells in DLN of IMQ-induced psoriasis-like model. (A-B) Representative flow cytometry diagrams and statistical analysis of Th1, Th2, Th17 and Treg cells among total CD4$^+$ T cells in the DLN of the IMQ-induced psoriasis mouse model treated with the ABT-737 gel (n=5) or vehicle gel (n=5). DLN, draining lymph nodes. Student's t test.

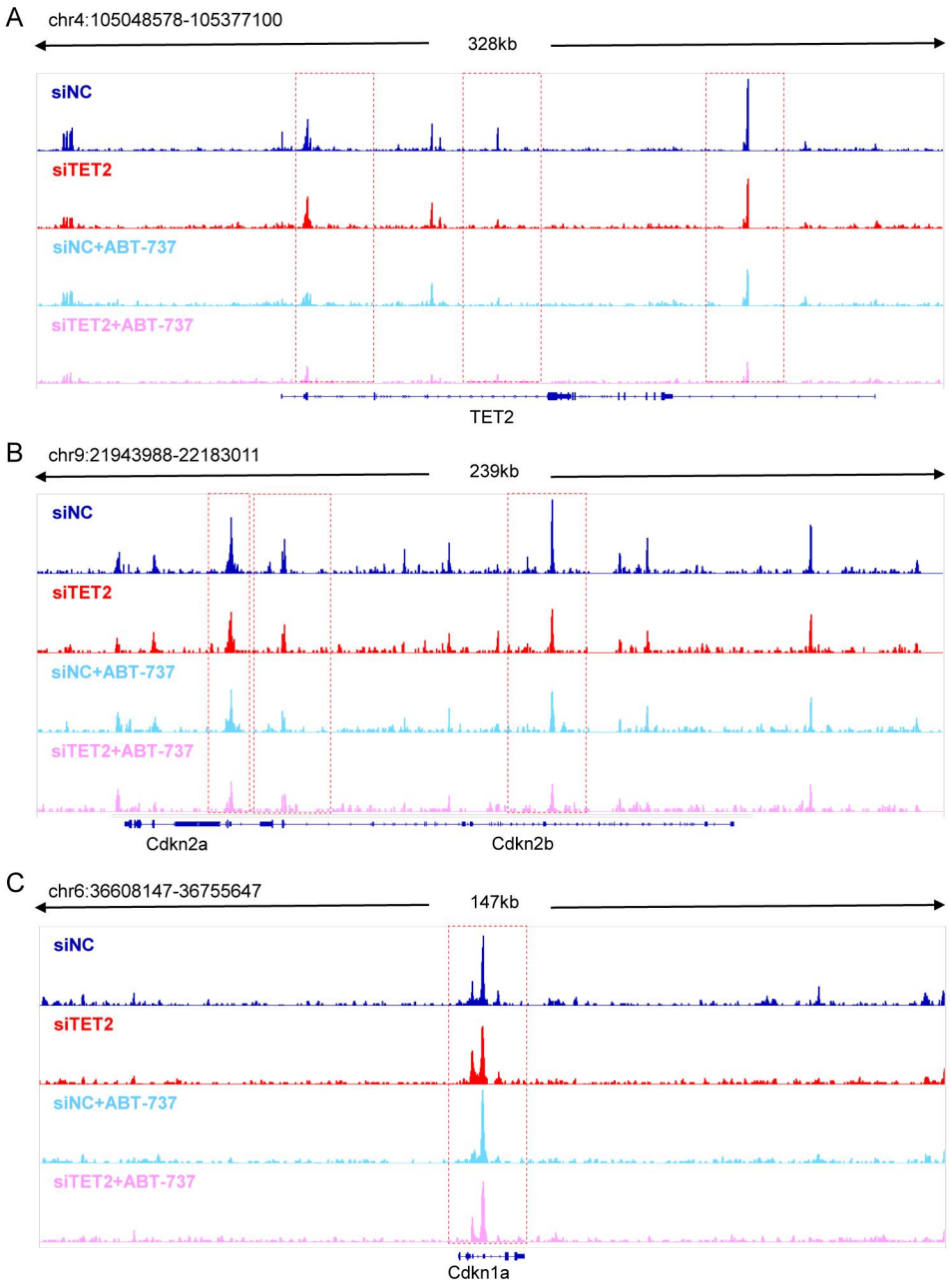

Figure S5. IGV browser tracks ATAC-seq in CD4+ T cell with siNC, siTET2, siNC+ABT-737, and siTET2+ABT-737 treatment along TET2 and senescence-related genes (*Cdkn2a, Cdkn2b*, and *Cdkn1a*).

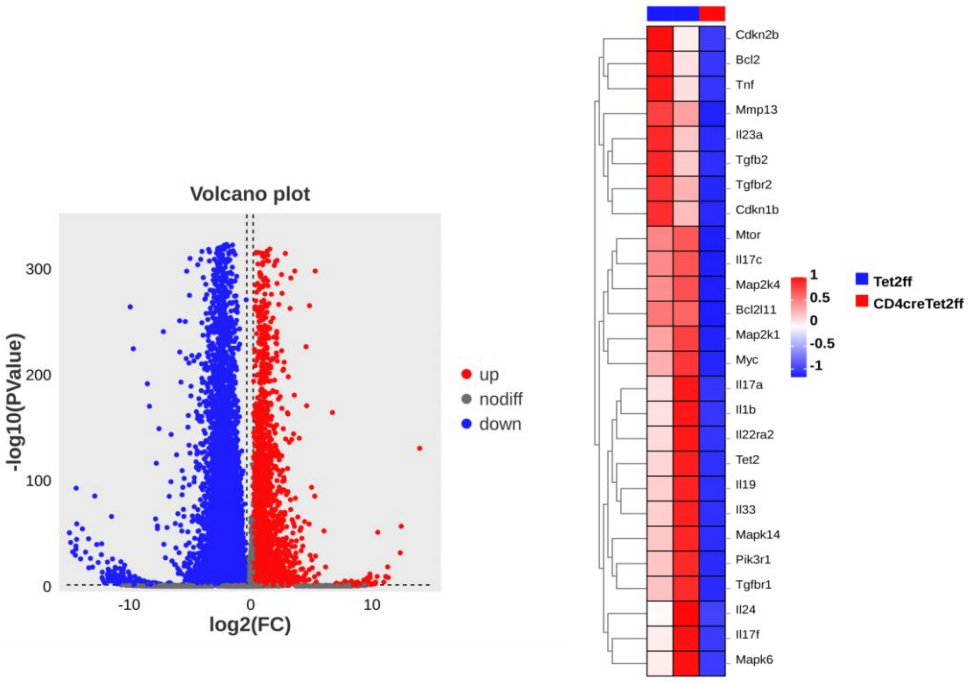

25

26 **Figure S6. Transcriptome comparison of CD4^{Cre}*Tet2*$^{f/f}$ and *Tet2* $^{f/f}$ mice skin lesions**

27

28

29 **Table S1 A. Information of psoriasis patients recruited.**

Number	Age	Sex	PASI
1	47	Male	10.4
2	61	Male	3.6
3	45	Male	4.0
4	53	Male	5.6
5	33	Male	10.0
6	59	Male	3.8
7	32	Male	10.4
8	42	Male	11.0
9	38	Male	0.9
10	33	Female	5.5
11	45	Male	10.0
12	50	Male	7.3
13	54	Female	7.6
14	55	Male	11.7
15	51	Male	5.6
16	35	Male	7.8
17	44	Male	9.0
18	65	Male	10.0

Table S1B. Information of healthy controls recruited.

Number	Age	Sex
1	59	Male
2	40	Male
3	78	Male
4	33	Male
5	48	Male
6	38	Male
7	27	Male
8	36	Female
9	33	Female
10	44	Female
11	40	Male
12	55	Male
13	54	Male
14	48	Male

Table S1C. Information of healthy controls recruited.

No.	Age	Sex	No.	Age	Sex
1	33	Male	4	36	Male
2	27	Female	5	39	Female
3	22	Female			

Table S2A. The sequence of PCR primers (Human).

	Forward primer	Reverse primer
IFNG	5'-GCAGAGCCAAATTGTCTCCTTT-3'	5'-TGTATTGCTTTGCGTTGGACA-3'
IL17A	5'-CTCTGTGATCTGGGAGGCAA-3'	5'-ACCAGTATCTTCTCCAGCCG-3'
IL21	5'-GGTCCACAAATCAAGCTCCC-3'	5'-TGGCAGAAATTCAGGGACCA-3'
p21	5'-GAAGTGAGCACAGCCTAG-3'	5'-TGCCTTCACAAGACAGAG-3'
$p16^{INK4a}$	5'-CTCCGGAAGCTGTCGACTTC-3'	5'-TTCTGCCATTTGCTAGCAGTGT-3'
IL6	5'-ACTCACCTCTTCAGAACGAATTG-3'	5'-CCATCTTTGGAAGGTTCAGGTTG-3'
IL8	5'-ACTGAGAGTGATTGAGAGTGGAC-3'	5'-AACCCTCTGCACCCAGTTTTC-3'
BCL2	5'-CCGAGATGTCCAGCCAGC-3'	5'-ACCCCACCGAACTCAAAGAA-3'
BCLxL	5'-GGAAAGCGTAGACAAGGAGATG-3'	5'-CCCGTAGAGATCCACAAAAGTG-3'
GAPDH	5'-GGAGCGAGATCCCTCCAAAAT-3'	5'-GGCTGTTGTCATACTTCTCATGG-3'

Table S2B. The sequence of PCR primers (Mouse).

	Forward primer	Reverse primer
Ifgγ	5’-AGACAATCAGGCCATCAGCA-3’	5’-CAACAGCTGGTGGACCACTC-3’
Il4	5’-GGTCTCAACCCCCAGCTAGT-3’	5’-GCCGATGATCTCTCTCAAGTGAT-3’
Il17a	5’-TTTAACTCCCTTGGCGCAAAA-3’	5’-CTTTCCCTCCGCATTGACAC-3’
Il17f	5’-GGAGGTAGCAGCTCGGAAGA-3’	5’-GGAGCGGTTCTGGAATTCAC-3’
Il22	5’-ATGAGTTTTTCCCTTATGGGGAC-3’	5’-GCTGGAAGTTGGACACCTCAA-3’
Il23	5’-AATAATGTGCCCCGTATCCAGT-3’	5’-GCTCCCCTTTGAAGATGTCAG-3’
p16^{INK4a}	5’-GAACTCTTTCGGTCGTACCC-3’	5’-AGTTCGAATCTGCACCGTAGT-3’
p21	5’-GAACATCTCAGGGCCGAAAA-3’	5’-TGCGCTTGGAGTGATAGAAATC-3’
Il6	5’-TAGTCCTTCCTACCCCAATTTCC-3’	5’-TTGGTCCTTAGCCACTCCTTC-3’
Tnfα	5’-CCCTCACACTCAGATCATCTTCT-3’	5’-GCTACGACGTGGGCTACAG-3’
Tet2	5’-AGAGAAGACAATCGAGAAGTCGG-3’	5’-CCTTCCGTACTCCCAAACTCAT-3’
Bcl2	5’-GAGCGTCAACAGGGAGATG-3’	5’-CAGAGACAGCCAGGAGAAATC-3’
BclxL	5’-GGAAAGCGTAGACAAGGAGATG-3’	5’-CCCGTAGAGATCCACAAAAGTG-3’
Klrg-1	5’-TTTGGGGCTTTTGACTGTGAT-3’	5’-TGTAAGGAGATGTGAGCCTTTGT-3’
Cd27	5’-CAGCTTCCCAACTCGACTGTC-3’	5’-GCACCCAGGACGAAGATAAGAA-3’
Cd28	5’-GTTCTTGGCTCTCAACTTCTTCT-3’	5’-TGAGGCTGACCTCGTTGCTAT-3’
Cdkn2b	5’-CCCTGCCACCCTTACCAGA-3’	5’-CAGATACCTCGCAATGTCACG-3’
Mtor	5’-ACCGGCACACATTTGAAGAAG-3’	5’-CTCGTTGAGGATCAGCAAGG-3’

RPLP0	5’-GAGACTGAGTACACCTTCCCAC-3’	5’-CCTCCGACTCTTCCTTTGCT-3’
GAPDH	5’-AGGTCGGTGTGAACGGATTTG-3’	5’-TGTAGACCATGTAGTTGAGGTCA-3’

Reference

1 **Wu, R., Zeng, J., Yuan, J., Deng, X., Huang, Y., Chen, L., Zhang, P., Feng, H., Liu, Z., Wang, Z., Gao, X., Wu, H., Wang, H., Su, Y., Zhao, M. and Lu, Q.,** MicroRNA-210 overexpression promotes psoriasis-like inflammation by inducing Th1 and Th17 cell differentiation. *J Clin Invest* 2018. **128**: 2551-2568.

2 **Zhao, Z., Zhu, H., Li, Q., Liao, W., Chen, K., Yang, M., Long, D., He, Z., Zhao, M., Wu, H. and Lu, Q.,** Skin CD4(+) Trm cells distinguish acute cutaneous lupus erythematosus from localized discoid lupus erythematosus/subacute cutaneous lupus erythematosus and other skin diseases. *J Autoimmun* 2022. **128**: 102811.

3 **Gallenne, T., Gautier, F., Oliver, L., Hervouet, E., Noel, B., Hickman, J. A., Geneste, O., Cartron, P. F., Vallette, F. M., Manon, S. and Juin, P.,** Bax activation by the BH3-only protein Puma promotes cell dependence on antiapoptotic Bcl-2 family members. *J Cell Biol* 2009. **185**: 279-290.

4 **Roliński, M., Montaldo, N. P., Aksu, M. E., Fordyce Martin, S. L., Brambilla, A., Kunath, N., Johansen, J., Erlandsen, S. E., Liabbak, N. B., Rian, K., Bjørås, M., Sætrom, P. and van Loon, B.,** Loss of Mediator complex subunit 13 (MED13) promotes resistance to alkylation through cyclin D1 upregulation. *Nucleic Acids Res* 2021. **49**: 1470-1484.

5 **Yang, Y., Wang, C., Yang, Q., Kantor, A. B., Chu, H., Ghosn, E. E., Qin, G., Mazmanian, S. K., Han, J. and Herzenberg, L. A.,** Distinct mechanisms define murine B cell lineage immunoglobulin heavy chain (IgH) repertoires. *Elife* 2015. **4**: e09083.

6 **Wu, J., Li, Y., Feng, D., Yu, Y., Long, H., Hu, Z., Lu, Q. and Zhao, M.,** Integrated analysis of ATAC-seq and RNA-seq reveals the transcriptional regulation network in SLE. *Int Immunopharmacol* 2023. **116**: 109803.